

Integrated Control of Operable Fenestration Systems and Thermally Massive HVAC Systems

Methods and Simulation Studies of Energy Savings Potential

Brian Coffey, Ph.D.
3331 Wildwood Rd, Kelowna, BC, V1W 2S3, Canada
brian.edward.coffey@gmail.com

As subcontractor to:
Eleanor S. Lee, PI
Windows and Envelope Materials Group
Building Technology and Urban Systems Department
Environmental Energy Technologies Division
Lawrence Berkeley National Laboratory
1 Cyclotron Road, Mailstop 90-3111
Berkeley, CA 94720

October 4, 2012

Technical Report
California Energy Commission Public Interest Energy Research (PIER) Program

Abstract

The future design of high performance buildings is expected to involve more active facade technologies, acting in intelligent collaboration with the HVAC and lighting systems to produce comfortable indoor environments with reduced energy consumption. Integrated control of active facade systems and HVAC is challenging, particularly with thermally-massive HVAC systems such as radiant floors and ceilings. This paper describes methods for devising near-optimal controllers for such integrated systems, allowing for any arbitrary level of complexity in the facade system. An offline-optimization approximation to model predictive control is used with a model consisting of a reduced-order approximation of the zone and HVAC thermal properties and an interpolation grid of the daylight and solar gains attributes of the facade in its various possible states. The optimization over the 24-hour prediction horizon is split into two levels, with GenOpt used at the top level to deal with the complexity of the facade, alongside a linear programming solution to the chilled slab control. The model can be calibrated to match monitored data, or some combination of whole-building energy modeling and Radiance outputs. To test the methods and to estimate energy savings potential, case studies were performed with a calibrated model based on an EnergyPlus ASHRAE 90.1-2010 office building, modified to use radiant slabs and operable Venetian blinds (either internal or external) or electrochromic glazing. Results are shown for four US climates. Further research is discussed.

Contents

1	Introduction	4
1.1	Motivations: The challenges and potential benefits of integrated facade-HVAC control	4
1.2	Model Predictive Control (MPC) description and history	4
1.2.1	MPC description	4
1.2.2	MPC in buildings	5
1.2.3	MPC for integrated control of facade-HVAC systems	5
1.2.4	Approximations to MPC for easier implementation	7
1.3	Research objectives and approach	9
2	Methods	10
2.1	Control optimization problem description	10
2.2	Models	10
2.2.1	EnergyPlus model	10
2.2.2	Why EnergyPlus + GenOpt cannot be used directly for this problem	11
2.2.3	Reduced-order model	12
2.2.4	Calibration of reduced-order model to match EnergyPlus model	16
2.3	Control optimization configuration	19
2.3.1	Two-level optimization problem configuration	19
2.3.2	Linear programming solution to cooling control subproblem	20
2.3.3	GenOpt solution to the overall problem with shading position	21
2.4	Offline optimizations over a grid of conditions	22
2.4.1	Conditions parametrization	22
2.4.2	Conditions grid definition and solution	22
2.5	Annual simulations	23
2.5.1	Configurations	23
2.5.2	Heuristic control cases for comparison	24
2.5.3	Two near-optimal controllers: ‘Lookup’ and ‘luOptCool’	25
2.5.4	Control block length in case studies	25
3	Simulation studies of savings potential: Case descriptions	26
3.1	Overview: Case study configurations	26
3.2	Fenestration system descriptions	27
3.2.1	Venetian blinds	27
3.2.2	Electrochromic windows	27
3.3	Reduced-order model descriptions	28
3.3.1	Shading grids	28
3.3.2	Thermal parameters	29
3.3.3	Schedules of internal loads and lighting setpoints	32

3.4	Lookup table calculation configurations	32
3.4.1	Conditions parametrization for lookup tables	32
4	Simulation studies of savings potential: Results	34
4.1	External Venetian blinds, South zone	34
4.1.1	Control lookup tables	34
4.1.2	Annual simulation details, Chicago case	37
4.1.3	Annual simulation results, all climates	39
4.2	External venetian blinds, West zone	42
4.2.1	Control lookup table	42
4.2.2	Annual simulation results	42
4.3	Internal venetian blinds, South zone	44
4.3.1	Control lookup table	44
4.3.2	Annual simulation results	44
4.4	Electrochromic windows, South zone	46
4.4.1	Control lookup table	46
4.4.2	Annual simulation results	46
4.5	Results summary	48
5	Discussion	50
5.1	Annual simulation results	50
5.2	Methods	51
5.2.1	Possible refinements to the controllers	51
5.2.2	Automating the methods for further studies and/or for market im- plementation	51
5.3	Other fenestration and HVAC systems to consider	52
5.4	Further research	52
6	Conclusions	53
7	Acknowledgments	54

1 Introduction

1.1 Motivations: The challenges and potential benefits of integrated facade-HVAC control

In all buildings, the envelope, lighting and HVAC systems work together to create an indoor environment that is different from the outdoors. The envelope is usually a relatively static, passive part of this process. In pushing towards very low energy buildings that meet contemporary comfort expectations, researchers and designers are increasingly considering envelope technologies that play a more active role. Intelligent control strategies for integrated systems of active facade, HVAC and lighting are essential not only for their effective implementation, but must also be considered within their design; the design of system components and system control go hand in hand, particularly for more innovative systems.

However, there are challenges associated with the integrated control of facade-HVAC-lighting systems, particularly in the case of thermally massive HVAC systems. For example, what does the optimal control response of an integrated shading and radiant cooling system look like? How much pre-cooling should happen and when, in order to cool less often when the ambient temperature is high and thus the cooling COP is low? And how should the shading system work in conjunction with this pre-cooling - when should it increase shading to decreasing cooling load but increase lighting load? The answers to such questions, it seems, are very much dependent on the configuration and properties of the building under consideration. Can we thus devise tools and techniques that can be used to provide custom answers to these questions for any particular building? How much energy savings potential is there with optimal integrated control of facade and HVAC systems?

This paper attempts to address these questions, if only incompletely. It builds upon previous research into Model Predictive Control (MPC) for building systems, describes a near-optimal controller development process that could be applied to a wide variety of systems involving either simple or complex fenestration systems in conjunction with radiant cooling and/or heating systems, and estimates energy savings potential by applying such controllers to annual simulations of ASHRAE 90.1-2010 based models of office buildings with radiant systems and either internal Venetian blinds, external Venetian blinds or electrochromic windows.

1.2 Model Predictive Control (MPC) description and history

1.2.1 MPC description

MPC is a repeated solution of a finite-time optimal control problem: at each controller time step, an optimal sequence of control values over a prediction horizon is calculated, only the first of which is implemented, and at the next controller time step the horizon shifts forward one step and the process is repeated. Note that in its standard form, the

optimization is performed online (in real time) within the controller, and that the control logic is implicit rather than explicit: the control designer must define the model and configure the optimization, but does not specify (or know in advance) what the control response will be under particular conditions.

MPC is well established in other fields. It was first used in the chemical process industry in the 1960s, and has seen increasing use since then. A survey by Qin and Badgwell [2003] notes that MPC is used in more than 4,000 industrial applications. It was a practically proven technique before it was studied theoretically, with investigations of stability and optimality criteria beginning in earnest in the 1980s. Overviews are available in Morari and Lee [1999] and Mayne et al. [2000], and the techniques encapsulated in a Matlab toolbox [MathWorks, 2012].

1.2.2 MPC in buildings

Buildings researchers have been investigating model-based controls for decades (e.g. Cumali [1988], Braun [1990], Keeney and Braun [1996], House and Smith [1996] and Flake [1998], Mahdavi [2001], Mahdavi et al. [2005], Mahdavi and Proglhof [2005], [Henze et al., 2004, 2005, Henze and Liu, 2005, Henze and Krarti, 2005, May-Ostendorp et al., 2011], [Kummert et al., 2005, Kummert and Andre, 2005], [Clarke et al., 2002], [Wang and Jin, 2000], [Nassif et al., 2005a,b]). There has been increasing interest in this research over the past decade, both as computation power has become more easily available, and as more complex supervisory control challenges have come up with system designers looking to find energy savings by integrating systems and/or by using low-energy HVAC systems often involving active thermal mass. Some recent work on MPC in buildings has also come from controls researchers from other fields turning their attention to buildings (e.g. Ma et al. [2010] and Oldewurtel et al. [2010]). A workshop in summer 2011 brought together many of the world's active researchers in this field [IBPSA-USA and IBPSA-Canada, 2011]. Potential for energy savings, demand reduction and performance improvement has been shown with a wide variety of systems, including chilled water storage, radiant slab pre-cooling and integrated HVAC and facade control. It has not yet, however, found its way into common practice within the industry.

1.2.3 MPC for integrated control of facade-HVAC systems

There are some examples of integrated facade-HVAC control with MPC in the literature (e.g. the work of Madhavi noted above), the most notable of which is a very extensive study called the OptiControl project carried out by ETH Zurich, Siemens and various partners [ETH-Zurich, 2011]. The project looked at various building systems and climates throughout Europe, including various levels of construction quality and variations on other parameters such as window area fraction. Some of their results are summarized in Table 1, with explanations of terms shown in Figures 1 and 2.

Table 1: Energy Savings Potential: Average (over all simulations in various European climates) annual total energy savings with perfect MPC (with perfect prediction and no modeling errors) versus best available rule-based control. Derived from results in Table 7.10 [Gyalistras and Gwerder, 2010]

Building System	Passive House Construction		Swiss Average Standard Construction		
	Type I	Type II	Type I	Type II	Type III
S1	12%	16%	9%	10%	7%
S2	9%	12%	7%	8%	6%
S3	6%	8%	7%	5%	4%
S4	1%	5%	1%	2%	1%
S5	15%	18%	12%	6%	-7%

Figure 1: ETH table 2.3

<i>Automated Subsystems</i>	<i>Building System</i>				
	<i>S1</i>	<i>S2</i>	<i>S3</i>	<i>S4</i>	<i>S5</i>
<i>Blinds</i>	x	x	x	x	x
<i>Electric lighting</i>	x	x	x	x	x
<i>Mechanical ventilation flow, heating, cooling</i>	–	x	x	x	x
<i>Mechanical ventilation energy recovery</i>	–	x	x	x	x
<i>Natural ventilation heating/cooling (night-time only)</i>	–	–	–	x	–
<i>Cooled ceiling (capillary tube system)</i>	x	x	–	–	–
<i>Free cooling with wet cooling tower</i>	x	x	–	–	x
<i>Radiator heating</i>	x	x	–	–	–
<i>Floor heating</i>	–	–	–	x	–
<i>Thermally activated building systems for heating/cooling</i>	–	–	–	–	x

Table 2.3: Building systems considered. “x” denotes the presence of a subsystem.

Figure 2: ETH table 2.2 (note that ‘pa’ represents ‘passive house’ and ‘sa’ represents ‘swiss average’)

<i>Building Standard</i>	<i>pa</i>				<i>sa</i>			
	<i>wh</i>		<i>wl</i>		<i>wh</i>		<i>wl</i>	
<i>Window Area Fraction</i>	<i>h</i>	<i>l</i>	<i>h</i>	<i>l</i>	<i>h</i>	<i>l</i>	<i>h</i>	<i>l</i>
<i>Construction Type</i>	<i>h</i>	<i>l</i>	<i>h</i>	<i>l</i>	<i>h</i>	<i>l</i>	<i>h</i>	<i>l</i>
<i>Façade Orientation</i>								
<i>N</i>	I	II	II	II	III	III	I	II
<i>S</i>	I	II	II	II	III	III	I	II
<i>SE</i>	II	II	II	II	III	III	II	II
<i>SW</i>	II	II	II	II	III	III	II	II

Table 2.2: Classification of building cases according to four key attributes. I: Common and wide-spread configurations; II: Less common configurations; III: Exotic cases. For abbreviations see Table 2.1.

For those interested in estimates of the energy savings potential with integrated control of blinds, lighting and HVAC systems, the OptiControl project is a good place to start. Their findings suggest that the most significant energy savings potential with MPC are for complex systems combined with thermal mass ¹ in climates and building designs with high and variable energy fluxes (e.g. solar). Our research hopes to complement the research in that project, with a greater focus on methods for developing easier-to-develop-and-implement near-optimal controls for systems involving either simple or complex fenestration systems, and with application to North American climates.

1.2.4 Approximations to MPC for easier implementation

There are three inherent aspects of the approach that are likely causing some of the gap between successful case-study demonstration and market uptake: (1) online optimization is difficult to implement with existing building control systems; (2) the control responses are implicit rather than explicit, which makes it difficult for system designers to integrate it into their design processes; and (3) it is difficult to use standard building simulation tools for MPC because of their long run-times and the fact that many do not allow the user to explicitly specify initial state values. For these reasons, and possibly for other reasons as well, some of the buildings MPC research has been carried out not with the goal of getting the methods themselves into common practice, but rather with an eye to developing near-optimal rules for some class of buildings by extrapolating from the results of optimal control studies with prototypical buildings. However, a major benefit of MPC is its ability to deal with innovative building systems customized to their contexts, for which generalized rules would likely not apply. As such, there is a continued push from researchers to make online-optimization MPC a marketable technology in buildings (e.g. [Sloup et al., 2011]), although at present it remains far from common practice in the industry. Previous research by the author has also attempted to facilitate the methods' uptake in design and operation through the development of an open-source software framework for online MPC [Coffey et al., 2010], using GenOpt [Wetter, 2009] as the optimization engine and thus allowing for the use of almost any common building simulation tool, which has been a key goal of the development: in addition to the benefits of user familiarity, using common building simulation tools for MPC could allow for the re-use of design phase models, and it could dovetail with other re-uses of these models to improve building operations through benchmarking, fault detection and diagnosis, and retrofit analysis. Recent work by May-Ostendorp et al. [2011] considers the approach of simulating online MPC over some or all of a representative year of disturbances (weather, occupancy, etc) and then using statistical techniques to derive near-optimal control laws from the results. This could provide a useful way of approaching the problem, but it will be difficult to parallelize the computation. An alternative approach, used herein, is to more explicitly map the optimal control responses

¹Note that high thermal mass cases were not found to have uniformly higher potential than low thermal mass cases, it depends on its combination with the other factors.

over the range of expected operational conditions (disturbances and initial states). We cannot compute the entire set of control responses directly, but we can approximate the optimal control response surface over the conditions range by sampling: calculating the optimal responses over some grid of points and then interpolating between them. The author’s recent dissertation [Coffey, 2011], attempted to clarify this approach and its range of applicability, for both steady-state and predictive problems, and investigated techniques to make it feasible for a broad range of problems with common building simulation tools. Figure 3 illustrates the structure used to produce near-optimal control lookup tables using a building simulation tool and GenOpt. Figure 4 shows the range of feasibility of the approach, based on computational budget.

Figure 3: Open-source software for producing near-optimal control lookup tables, can use most existing building modeling software

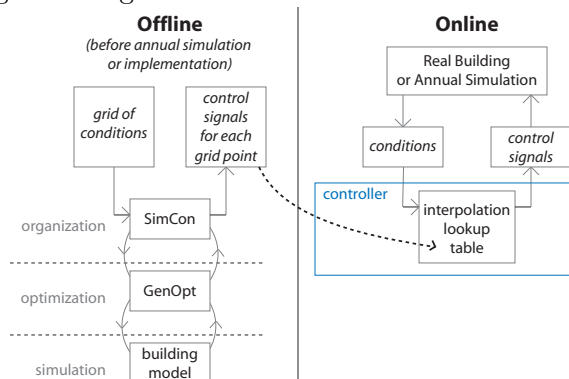
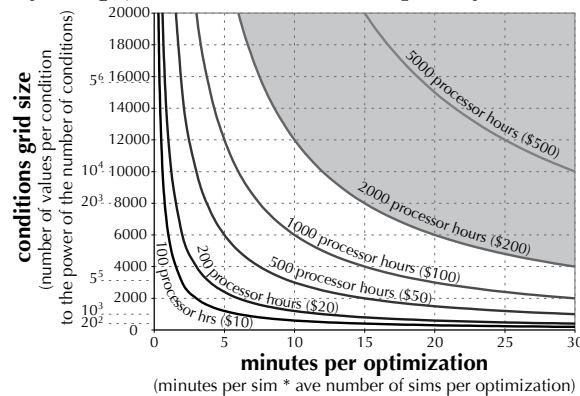


Figure 4: Feasibility range, based on model complexity and conditions grid size



Essentially, we want to enable buildings researchers, designers and product developers to use their existing software and models for energy analysis, with limited additional skills

development, to develop near-optimal controls for systems both for implementation, and for use within the design process. Open-source software has been developed in previous research for use with any type of systems. It has been more fully tested and fleshed out herein within the particular context of facade-lighting-HVAC integration.

To the author’s knowledge there are no research precedents of offline-optimization control lookup table construction for integrated facade-HVAC-lighting systems, aside from two case studies in [Coffey, 2011]: one looking at the integrated control of a theoretical system of shading and natural ventilation, and one looking at a system of internal Venetian blind shading and UFAD (also reported in [Coffey and Lee, 2011]).

1.3 Research objectives and approach

The research described herein aims to develop tools and methods for deriving near-optimal controllers for simple or complex fenestration systems coupled with thermally massive radiant heating and cooling systems, and to estimate their energy savings potential by applying them to annual simulations of case study buildings in various North American climates.

As described in more detail below, in all of the cases a 24 hour prediction horizon is being used and a 1 hour control timestep applied to both the shade position and the cooling level (or, equivalently, the zone temperature setpoint). As such, the control optimization problem is too large to be dealt with directly by using GenOpt and EnergyPlus, as might be hoped. A simplified model is developed herein, which includes a reduced-order thermal model that may be calibrated to an EnergyPlus model (or any other thermal model, or to measured data), and a fenestration component that may be of any arbitrary level of complexity. Splitting the model into these parts will allow us to investigate the control of innovative complex fenestration systems, while the reduced-order thermal part of the model allows for faster optimizations.

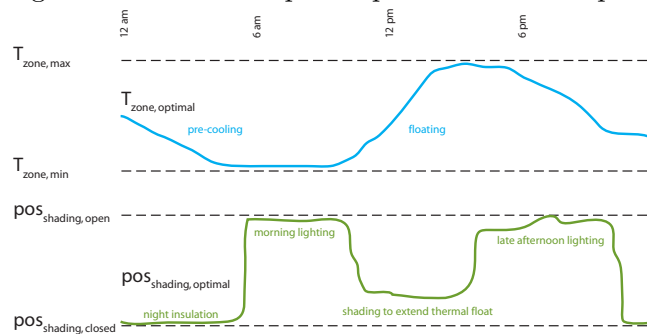
The next section describes the methods, followed by some case study results with internal Venetian blinds, external Venetian blinds and electrochromic windows. The applicability of the results and methods are discussed thereafter, along with next steps in future research.

2 Methods

2.1 Control optimization problem description

At any given time t , the controller must determine the shading position u_{shade} and radiant cooling level u_{cool} (or, equivalently, the zone temperature setpoint T_{zoneSP}) to minimize energy consumption for lighting and cooling, $Q_{consumed}$, over a prediction horizon of 24 hrs, subject to zone temperature constraints, and given weather conditions and predictions. The zone temperature is constrained as follows: at any hour in the simulation, $T_{zone} > T_{zoneMin}$ or $T_{zone} < T_{zoneMax}$ (where $T_{zoneMin}$ is set to 20C and $T_{zoneMax}$ is set to 24C). Figure 5 illustrates a possible optimal control response over a day.

Figure 5: Possible shape of optimal control response

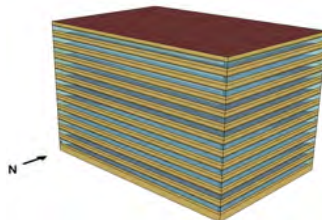


2.2 Models

2.2.1 EnergyPlus model

The EnergyPlus model used for the case studies was based on the PNNL Large Office ASHRAE 90.1-2010 compliant EnergyPlus model. These models were created and used by PNNL to test the energy savings between 90.1-2007 and 90.1-2010, and then posted online as reference models. An image of the model (from the model descriptions in the download) is shown in Figure 6. The building is 240' x 160', with a perimeter zone depth of 15'.

Figure 6: PNNL Large Office ASHRAE 90.1-2010 compliant prototype model



The model’s HVAC system was modified for this research. The VAV system was turned off, and a radiant slab heating and cooling system was added in its place. The radiant tube depth was set to 5cm, the tube spacing to 6” and inside tube diameter to 0.5”. The tube length was set to the floor area divided by the tube spacing. The flow rate was sized manually to provide a peak capacity of 25 W/sqft (assuming 12C between supply and return water temperatures). The radiant system is set to control to a zone temperature setpoint, which is generally achieved with a minor time lag.

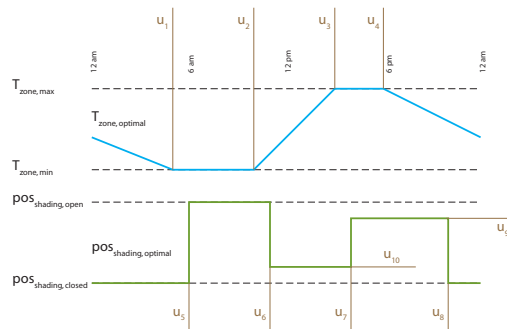
External Venetian blinds, internal Venetian blinds or electrochromic windows were also added to the model, depending on the case. The Venetian blinds are modeled as being always deployed, with just their slat angle changing over time. The details of the window and shading systems are described in the case study descriptions below.

The main control variables of interest for each zone are the zone air temperature setpoint and the shading position (or electrochromic level of shading). The middle story of the building was used for this study.

2.2.2 Why EnergyPlus + GenOpt cannot be used directly for this problem

The control optimization problem is simply too big. With a 24 hour prediction horizon, two control variables and an hourly control timestep, there are 48 optimization variables to consider at each control timestep. Setting u_{shade} to a constant when the sun is down would eliminate some of the optimization variables, but still leaves roughly 40 in the worst case. This is too many variables to be tractable with EnergyPlus and GenOpt. If the problem could be reconfigured and/or simplified to involve fewer optimization variables without losing significant accuracy, then it could possibly be made tractable. But there is no obvious way of doing so. Figure 5 shows a possible daily shape of the optimal control response, which is likely to occur in some cases but not all. If one was confident enough that this shape would occur all or most of the time, it could be approximated as shown in Figure 7, reducing the optimization problem to just 10 variables. However, without more detailed studies of the optimal control, it is difficult to justify such an approximation.

Figure 7: Possible parametrization of control response



Model implementation in Java

The model was coded in Java to avoid the computational time overhead associated with tools like Trnsys or Modelica, to allow it to be run on any operating system without license problems, thus enabling its use with cloud computing. A closed-form solution to the system of differential equations (Equations 4 and 5) was produced and the model coded in Java. This allows the simulation to run without any convergence loops. The derivation of the system of equations and its solution are shown below. For convenience of notation, the following name assignments are made.

$$\begin{aligned}
 x_1 &\leftarrow T_{zone}, & x_2 &\leftarrow T_{slab} \\
 \alpha_1 &\leftarrow \frac{UA_{zone}}{C_{zone}}, & \alpha_2 &\leftarrow \frac{h_c}{C_{zone}}, & \alpha_3 &\leftarrow \frac{h_c}{C_{slab}} \\
 \beta_1 &\leftarrow \frac{UA_{zone}T_{amb} + Q_{solZone} + Q_{occEquip} + Q_{AL}}{C_{zone}}, & \beta_2 &\leftarrow \frac{Q_{solSlab}}{C_{slab}}, & \beta_3 &\leftarrow \frac{Q_{coolMax}}{C_{slab}}
 \end{aligned} \tag{7}$$

Note that the system of differential equations (Equations 4 and 5) can be represented in the form shown in Equation 8

$$\dot{\mathbf{x}} = \mathbf{A}\mathbf{x} + \mathbf{B}\mathbf{u} \tag{8}$$

where

$$\mathbf{x} = \begin{bmatrix} x_1 \\ x_2 \end{bmatrix}, \quad \mathbf{u} = \begin{bmatrix} u_1 \\ 1 \end{bmatrix}, \quad \mathbf{A} = \begin{bmatrix} -\alpha_1 - \alpha_2 & \alpha_2 \\ \alpha_3 & -\alpha_3 \end{bmatrix}, \quad \mathbf{B} = \begin{bmatrix} 0 & \beta_1 \\ -\beta_3 & \beta_2 \end{bmatrix} \tag{9}$$

The solution to Equation 8 at any time t is as follows.

$$\mathbf{x}(t) = e^{t\mathbf{A}}\mathbf{x}(0) + \int_0^t \left(e^{(t-\iota)\mathbf{A}}\mathbf{B}\mathbf{u} \right) d\iota \tag{10}$$

The integration and matrix calculations were carried out using Mathematica to produce Equations 12 and 13. Further variable name assignments are provided below to simplify the equations.

$$\begin{aligned}
 \kappa_1 &\leftarrow \alpha_1 + \alpha_2 + \alpha_3, & \kappa_2 &\leftarrow \alpha_1 + \alpha_2 - \alpha_3 \\
 \kappa_3 &\leftarrow \sqrt{-4\alpha_1\alpha_3 + (\alpha_1 + \alpha_2 + \alpha_3)^2}, & \kappa_4 &\leftarrow \sqrt{\alpha_1^2 + 2\alpha_1(\alpha_2 - \alpha_3) + (\alpha_2 + \alpha_3)^2}
 \end{aligned} \tag{11}$$

$$\begin{aligned}
x_1(t + \tau) = & x_2(t) \left(\frac{-\alpha_2 e^{\frac{1}{2}\tau(-\kappa_1 - \kappa_3)} + \alpha_2 e^{\frac{1}{2}\tau(-\kappa_1 + \kappa_3)}}{\kappa_3} \right) \\
& + x_1(t) \left(\frac{-e^{\frac{1}{2}\tau(-\kappa_1 - \kappa_3)}(-\kappa_2 - \kappa_3) + e^{\frac{1}{2}\tau(-\kappa_1 + \kappa_3)}(-\kappa_2 - \kappa_3)}{2\kappa_3} \right) \\
& + \frac{1}{2\kappa_3} \left(\frac{-2 \left(1 - e^{\frac{-1}{2}\tau(\kappa_1 + \kappa_4)} \right) (\kappa_2 \beta_1 + \kappa_4 \beta_1 - 2\alpha_2 \beta_2 + 2u_1 \alpha_2 \beta_3)}{\kappa_1 + \kappa_4} \right. \\
& \quad \left. - \frac{2 \left(-1 + e^{\frac{-1}{2}\tau(\kappa_1 - \kappa_4)} \right) (-\kappa_2 \beta_1 + \kappa_4 \beta_1 + 2\alpha_2 \beta_2 - 2u_1 \alpha_2 \beta_3)}{\kappa_1 - \kappa_4} \right) \tag{12}
\end{aligned}$$

$$\begin{aligned}
x_2(t + \tau) = & x_1(t) \left(\frac{-\alpha_3 e^{\frac{1}{2}\tau(-\kappa_1 - \kappa_3)} + \alpha_3 e^{\frac{1}{2}\tau(-\kappa_1 + \kappa_3)}}{\kappa_3} \right) \\
& + x_2(t) \left(\frac{-e^{\frac{1}{2}\tau(-\kappa_1 - \kappa_3)}(\kappa_2 - \kappa_3) + e^{\frac{1}{2}\tau(-\kappa_1 + \kappa_3)}(\kappa_2 - \kappa_3)}{2\kappa_3} \right) \\
& + \frac{1}{2\kappa_3} \left(\frac{2 \left(1 - e^{\frac{-1}{2}\tau(\kappa_1 + \kappa_4)} \right) ((-\alpha_1 - \alpha_2 + \kappa_4)(\beta_2 - u_1 \beta_3) + \alpha_3(-2\beta_1 + \beta_2 - u_1 \beta_3))}{\kappa_1 + \kappa_4} \right. \\
& \quad \left. - \frac{2 \left(-1 + e^{\frac{-1}{2}\tau(\kappa_1 - \kappa_4)} \right) ((\alpha_1 + \alpha_2 + \kappa_4)(\beta_2 - u_1 \beta_3) + \alpha_3(2\beta_1 - \beta_2 + u_1 \beta_3))}{\kappa_1 - \kappa_4} \right) \tag{13}
\end{aligned}$$

This can be simplified to the form shown in Equations 22 and 23, with the values of Γ_i defined in Equations 14 through 21. Note that only Γ_4 and Γ_8 are time-variant, since only β_1 and β_2 are time-variant.

The model was formulated with the cooling profile (\mathbf{u}_{cool}) as the expected input, but through further manipulations of Equations 22 and 23, one can determine the required cooling profile to produce a desired zone temperature profile (\mathbf{x}_1). This allows the model to effectively be used with either a cooling profile or a zone temperature profile as the input.

Although the model is formulated in continuous time, it is simulated in discrete time (with a fixed value of τ). Any desired timestep τ can be used; for the cases described herein, a simulation timestep of 1 hour is used throughout.

$$\Gamma_1 \leftarrow \left(\frac{-e^{\frac{1}{2}\tau(-\kappa_1-\kappa_3)}(-\kappa_2-\kappa_3) + e^{\frac{1}{2}\tau(-\kappa_1+\kappa_3)}(-\kappa_2-\kappa_3)}{2\kappa_3} \right) \quad (14)$$

$$\Gamma_2 \leftarrow \left(\frac{-\alpha_2 e^{\frac{1}{2}\tau(-\kappa_1-\kappa_3)} + \alpha_2 e^{\frac{1}{2}\tau(-\kappa_1+\kappa_3)}}{\kappa_3} \right) \quad (15)$$

$$\Gamma_3 \leftarrow \frac{-1}{\kappa_3} \left(\frac{\left(1 - e^{-\frac{1}{2}\tau(\kappa_1+\kappa_4)}\right)(2\alpha_2\beta_3)}{\kappa_1 + \kappa_4} - \frac{\left(1 - e^{-\frac{1}{2}\tau(\kappa_1-\kappa_4)}\right)(-2\alpha_2\beta_3)}{\kappa_1 - \kappa_4} \right) \quad (16)$$

$$\Gamma_4(t) \leftarrow \frac{-1}{\kappa_3} \left(\frac{\left(1 - e^{-\frac{1}{2}\tau(\kappa_1+\kappa_4)}\right)(\kappa_2\beta_1 + \kappa_4\beta_1 - 2\alpha_2\beta_2)}{\kappa_1 + \kappa_4} - \frac{\left(1 - e^{-\frac{1}{2}\tau(\kappa_1-\kappa_4)}\right)(-\kappa_2\beta_1 + \kappa_4\beta_1 + 2\alpha_2\beta_2)}{\kappa_1 - \kappa_4} \right) \quad (17)$$

$$\Gamma_5 \leftarrow \left(\frac{-\alpha_3 e^{\frac{1}{2}\tau(-\kappa_1-\kappa_3)} + \alpha_3 e^{\frac{1}{2}\tau(-\kappa_1+\kappa_3)}}{\kappa_3} \right) \quad (18)$$

$$\Gamma_6 \leftarrow \left(\frac{-e^{\frac{1}{2}\tau(-\kappa_1-\kappa_3)}(\kappa_2-\kappa_3) + e^{\frac{1}{2}\tau(-\kappa_1+\kappa_3)}(\kappa_2-\kappa_3)}{2\kappa_3} \right) \quad (19)$$

$$\Gamma_7 \leftarrow \frac{1}{\kappa_3} \left(\frac{\left(1 - e^{-\frac{1}{2}\tau(\kappa_1+\kappa_4)}\right)((-\alpha_1 - \alpha_2 + \kappa_4)(-\beta_3) + \alpha_3(-\beta_3))}{\kappa_1 + \kappa_4} - \frac{\left(-1 + e^{-\frac{1}{2}\tau(\kappa_1-\kappa_4)}\right)((\alpha_1 + \alpha_2 + \kappa_4)(-\beta_3) + \alpha_3(\beta_3))}{\kappa_1 - \kappa_4} \right) \quad (20)$$

$$\Gamma_8(t) \leftarrow \frac{1}{\kappa_3} \left(\frac{\left(1 - e^{-\frac{1}{2}\tau(\kappa_1+\kappa_4)}\right)((-\alpha_1 - \alpha_2 + \kappa_4)(\beta_2) + \alpha_3(-2\beta_1 + \beta_2))}{\kappa_1 + \kappa_4} - \frac{\left(-1 + e^{-\frac{1}{2}\tau(\kappa_1-\kappa_4)}\right)((\alpha_1 + \alpha_2 + \kappa_4)(\beta_2) + \alpha_3(2\beta_1 - \beta_2))}{\kappa_1 - \kappa_4} \right) \quad (21)$$

$$x_1(t + \tau) = \Gamma_1 x_1(t) + \Gamma_2 x_2(t) + \Gamma_3 u_1(t) + \Gamma_4(t) \quad (22)$$

$$x_2(t + \tau) = \Gamma_5 x_1(t) + \Gamma_6 x_2(t) + \Gamma_7 u_1(t) + \Gamma_8(t) \quad (23)$$

2.2.4 Calibration of reduced-order model to match EnergyPlus model

The reduced-order model can be calibrated to match an EnergyPlus model in two independent steps: (1) produce the lookup table for the shading device (f_1), and (2) calibrate the parameters associated with the thermal aspects of the model (UA_{zone} , h_c , $c_{zoneCap}$, $c_{slabCap}$).

Constructing the shading lookup table

The model equation 1, shown again below, relates the daylight level and solar gains on the slab and the zone air to the shade position and the outdoor conditions - solar position (via the ‘day’ and ‘hr’ variables), direct normal radiation and diffuse horizontal radiation.

$$[\dot{Q}_{solZone}, \dot{Q}_{solSlab}, lux_{DL}] = f_1(u_{shade}, day, hr, \dot{Q}_{direct}, \dot{Q}_{diffuse})$$

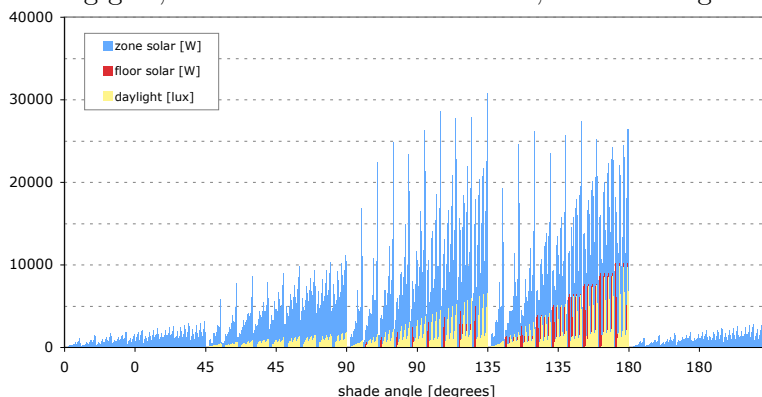
Given a building model, this function can be approximated as an interpolation lookup table, constructed by iteratively running the model over a grid of values for u_{shade} , day, hr, \dot{Q}_{direct} and $\dot{Q}_{diffuse}$. This process may be automated, given an EnergyPlus model, as follows:

1. Create a copy of the idf file.
2. Make sure the new idf file has the appropriate output variables listed: daylight level at sensor position, absorbed solar on the slab, zone window transmitted solar, window heat gain and window heat loss (the latter two are discussed further below).
3. Remove the RunPeriod object(s). Replace it with a set of RunPeriod objects for each day in the grid.
4. Identify the shade position variable within the idf file (this step requires user input, but that may be done up front), and produce a set of idf files (or iteratively overwrite one file as the process moves along) corresponding to all of the shade positions in the grid.
5. Create a set of epw files based on the given epw file, one for each combination of \dot{Q}_{direct} and $\dot{Q}_{diffuse}$ in the grid. This can be done by simply overwriting the entire direct and diffuse radiation columns in the epw file.
6. Run the large group of simulations for each combination of u_{shade} , \dot{Q}_{direct} and $\dot{Q}_{diffuse}$ in the grid.
7. Read the desired EnergyPlus outputs from these simulations ($\dot{Q}_{solZone}$, $\dot{Q}_{solSlab}$, lux_{DL}) into the desired form of the lookup table, associating them to the parameter values used to produce them.

Note that the value of $\dot{Q}_{solZone}$ must include the forward fraction of the solar gains on the window itself. This quantity is not easily obtained from EnergyPlus. A simple work-around is to simulate the model twice, once with zero radiation in the weather file, and once with the desired radiation for the point under consideration. In both cases, output the window heat gain and loss variables. The window heat gain and loss variables include the all of the transmitted solar gains, the forward fraction of the absorbed solar, and the conduction gains/losses. Ignoring any minor differences in conductive gains between the two cases caused by the different internal zone temperatures, one can remove the conductive gains/losses from the desired case by subtracting the total window heat gain/loss from the zero radiation case.

The reduced-order model was calibrated as described above for each of the climates and fenestration systems under consideration. For the shade gridding (f_1), the shade angle was varied over the values { 0 deg (fully down, closed), 45 deg, 90 deg (horizontally open), 135 deg, 180 deg (fully up, closed) } corresponding to { 0, 0.25, 0.5, 0.75, 1 } as the shading signal, direct radiation over values of { 0, 100, 200, 300, 400, 500, 600, 700, 800 } W/m², diffuse radiation over values of { 0, 100, 200, 300 } W/m², dayOfYear over 5 values between winter and summer solstice, and hrOfDay over the values { 6, 9, 12, 15, 18, 21 }. Figure 9 shows the results of the shading grid for the case of South-facing external Venetian blinds in Chicago - the vertical axis shows the outputs (in W or lux), the horizontal axis shows each line of the lookup table file. One can see five main divisions in the graph - these correspond to the shade angles. So in this case the shade angle of 90° has the highest gains (as expected), followed by the 135° angle. Within each of the five divisions, the direct and diffuse values are increasing, and the influence on the output values is roughly linear.

Figure 9: Shading grid, external Venetian blind case, South-facing zone, Chicago



Calibrating the thermal aspects of the model

The thermal aspects of model are more properly calibrated through an error-minimization calibration process. The differential equations in the model (Equations 5 and 6, shown again below) describe the progression of the zone and slab temperatures (T_{zone} , T_{slab}) over time, as a function of their initial states (T_{zone0} , T_{slab0}), the disturbances (T_{amb} , $\dot{Q}_{solZone}$, $\dot{Q}_{occEquip}$, \dot{Q}_{AL} , $\dot{Q}_{solSlab}$), the cooling input ($\dot{Q}_{cooling}$, considered as a given during calibration), and four parameters: UA_{zone} , h_c , $c_{zoneCap}$, and $c_{slabCap}$.

$$c_{zoneCap} \cdot \frac{dT_{zone}}{dt} = UA_{zone}(T_{amb} - T_{zone}) + h_c(T_{slab} - T_{zone}) + \dot{Q}_{solZone} + \dot{Q}_{occEquip} + \dot{Q}_{AL}$$

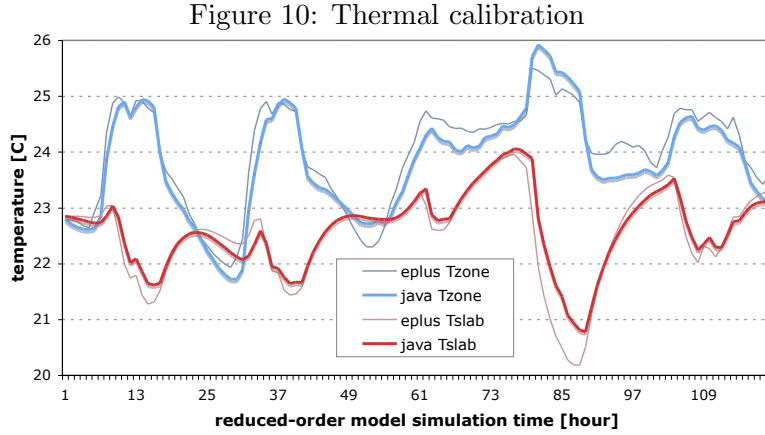
$$c_{slabCap} \cdot \frac{dT_{slab}}{dt} = h_c(T_{slab} - T_{zone}) + \dot{Q}_{solSlab} - \dot{Q}_{cooling}$$

The calibration is performed as follows:

1. Run EnergyPlus over some arbitrary period of time (e.g. 5 days in June and July were used in the case study below), with the following output variables listed in the idf: T_{amb} , $\dot{Q}_{solZone}$, $\dot{Q}_{occEquip}$, \dot{Q}_{AL} , $\dot{Q}_{solSlab}$, T_{zone} , T_{slab} and $\dot{Q}_{cooling}$.³
2. Process the outputs (including T_{zone0} and T_{slab0} , but not the rest of the T_{zone} and T_{slab} values) into a format appropriate to the reduced order model.
3. Wrap the reduced order model with GenOpt (i.e. set up the proper template file and config files, etc), with a model post-processor to compare the reduced-order model outputs of T_{zone} and T_{slab} over the horizon with those from the EnergyPlus, outputting the RMSE (root mean squared error) to a text file that is read by GenOpt as the objective function.
4. Run GenOpt to minimize the RMSE, with UA_{zone} , h_c , $c_{zoneCap}$, and $c_{slabCap}$ as the optimization variables. The optimal values of these variables are the calibrated values to use for the model.

Note that although the optimization is for just 4 variables, the objective function is complex and may have various local minima. Good initial points for the optimization can be easily defined based on the floor area of the zone under consideration. This helps to both speed up the optimization and to ensure that the results are reasonable.

Figure 10 shows a comparison of the EnergyPlus zone and slab temperature outputs for June 21-26, Chicago with those from the reduced-order model. The calibrated parameter values are shown in the case studies below in Table 4.



³This $\dot{Q}_{cooling}$ value from EnergyPlus proved a hassle, and in the end it was found by a barrage of tests that the EnergyPlus model to be somehow over-reporting the slab cooling amount by roughly 1.5 times. (This was not discovered until after other possible unaccounted-for heat sources were investigated, including the addition of the $\dot{Q}_{solZoneOpaque}$ model element.) In the end, a proxy for this value had to be used based on other EnergyPlus outputs.

2.3 Control optimization configuration

At any given point in time, the integrated shading-cooling controller is faced with the optimization problem noted earlier:

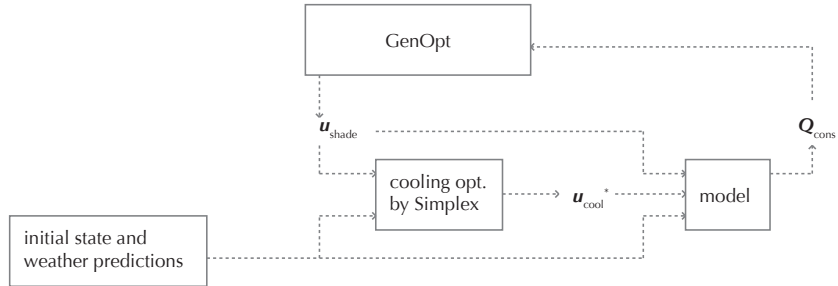
$$\begin{aligned}
 \min_{\mathbf{u}_{shade}, \mathbf{u}_{cool}} \quad & Q_{consumed} \\
 \text{s.t.} \quad & T_{zone_t} > T_{zoneMin}, t = 1..24 \\
 & T_{zone_t} < T_{zoneMax}, t = 1..24
 \end{aligned} \tag{24}$$

This optimization configuration uses the reduced-order model in the objective function. The 48-variable optimization can be solved directly using GenOpt by using penalty functions to keep the zone temperature within its boundaries. However, the GenOpt optimization is very computationally expensive and/or imprecise. So an attribute of the model’s structure is used to advantage as described below.

2.3.1 Two-level optimization problem configuration

The optimization problem can be split into two parts. The parts are not independent, but splitting them allows for an efficient solution method using a combination of GenOpt and a linear programming algorithm. The split follows the lines of the model, where the impact of the fenestration system is calculated first and then the resulting lighting requirements and solar gains are fed to the thermal network part of the model. The fenestration system is allowed to be of any arbitrary level of complexity within the model, while the thermal network is described as a linear system of differential equations. As described in the next section, given any shading position profile over the prediction horizon, the optimal cooling profile may be solved as a linear program using the Simplex algorithm. The complete control optimization problem, including the shading profile, cannot however be solved as a linear program because the fenestration system is nonlinear. So the overall problem is solved using GenOpt, with the cooling optimization subproblem solved within GenOpt’s objective function evaluation, as shown in Figure 11. The subproblem is thus solved many times in the process of finding the overall solution.

Figure 11: Two-level optimization problem configuration



This split will also be seen in variants on the implementation, including the use of a lookup table approximation of the higher-level problem to determine \mathbf{u}_{shade} combined with an online linear programming optimization of the subproblem to determine \mathbf{u}_{cool} .

The next section describes the subproblem solution using linear programming, followed by a description of the GenOpt configuration for the overall problem. The reader uninterested in these details may skip the following section without a significant loss in understanding the overall picture.

2.3.2 Linear programming solution to cooling control subproblem

The cooling optimization problem may be formulated as a linear program, and thus solved quickly and exactly by using the Simplex algorithm. The linear optimization problem in its standard format is shown in Equation 25, where the objective function vector \mathbf{c} is of length 24 (i.e. the same length as \mathbf{u}_{cool}), \mathbf{b} is a vector of length n , and \mathbf{A} is a matrix of dimension $24 \times n$, where n is the number of constraints.

$$\begin{aligned} \min_{\mathbf{u}_{cool}} \quad & \mathbf{c} \cdot \mathbf{u}_{cool} \\ \text{s.t.} \quad & \mathbf{A}\mathbf{u}_{cool} \leq \mathbf{b} \end{aligned} \tag{25}$$

The objective function vector \mathbf{c} is simply defined from the model equations, as shown in Equation 26.

$$c[t] = \frac{Q_{coolMax}}{COP[t]}, \text{ for } t = 1..24 \tag{26}$$

Parts of the constraint matrix \mathbf{A} and constraint vector \mathbf{b} are simple, given the box constraints on the control signal between 0 and 1.

$$u_{cool}[t] \leq 1 \tag{27}$$

$$-u_{cool}[t] \leq 0 \tag{28}$$

The challenge, however, is that the constraints on the zone temperature (a state variable) must be converted to constraints on the variables $u_{cool}[t]$. To do so, the equations must be rearranged to show the zone temperatures $x_1[t], t = 1..24$ and slab temperatures $x_2[t], t = 1..24$ as a function of the given Γ_i values, the initial temperatures $x_1[0], x_2[0]$ and the cooling control optimization variables $u_{cool}[t]$. This may be done by defining $q_1[t], q_2[t], w_1[i][t]$ and $w_2[i][t]$, for $t = 0..24$, as shown in Equations 29 and 30, and noting that their equations may be derived iteratively as shown by the algorithm labeled 31.

$$x_1[t] = q_1[t] + \sum_{i=0}^t (w_1[i][t] \cdot u_{cool}[i]) \tag{29}$$

$$x_2[t] = q_2[t] + \sum_{i=0}^t (w_2[i][t] \cdot u_{cool}[i]) \tag{30}$$

$$\begin{aligned}
&\text{set } q_1[0] \leftarrow x_1[0] \\
&\text{set } q_2[0] \leftarrow x_2[0] \\
&\text{for } t = 1..24 \quad q_1[t+1] = \Gamma_1 q_1[t] + \Gamma_2 q_2[t] + \Gamma_4[t] \\
&\quad \quad \quad q_2[t+1] = \Gamma_5 q_1[t] + \Gamma_6 q_2[t] + \Gamma_8[t] \\
&\quad \quad \quad w_1[t+1][t+1] = \Gamma_3[t+1] \\
&\quad \quad \quad w_2[t+1][t+1] = \Gamma_7[t+1] \\
&\quad \text{for } i = 0..t \quad w_1[i][t+1] = \Gamma_1 w_1[i][t] + \Gamma_2 w_2[i][t] \\
&\quad \quad \quad w_2[i][t+1] = \Gamma_5 w_1[i][t] + \Gamma_6 w_2[i][t]
\end{aligned} \tag{31}$$

Note that the problem constraints specify that $x_1[t] \leq x_{1_{max}}, \forall t$ (where $x_{1_{max}} = 24^\circ\text{C}$ in this implementation). Therefore, given Equation 29, the following is an equivalent constraint on the values of u_{cool_t} .

$$\sum_{i=0}^t (w_1[i][t] \cdot u_{cool}[i]) \leq x_{1_{max}} - q_1[t] \tag{32}$$

The constraints in Equations 27, 28 and 32 thus allow for the construction of the constraint matrix \mathbf{A} and constraint vector \mathbf{b} . Note that more constraints could be added, such as a lower bound for the zone temperature, or bounds on the slab temperature, by using similar manipulations of the equations.

2.3.3 GenOpt solution to the overall problem with shading position

Instead of calling the reduced-order model directly, GenOpt calls a small program that first calls the cooling optimizer, then passes the optimal cooling setpoints along with GenOpt's shading setpoints to the model, as shown in Figure 11. The GenOpt problem is otherwise a relatively straightforward optimization problem with 24 variables (just the shading variables over the horizon). The GPS-Hookes-Jeeves algorithm in GenOpt was used in the case studies below, with 2 step size reductions, to a control signals precision of 0.25.

2.4 Offline optimizations over a grid of conditions

The overall methods employed here are the same as those employed in [Coffey, 2011]. Given a model of the building / system under consideration, a grid of conditions is constructed to cover the range of current and predicted weather, occupancy and initial state conditions that the building / system is expected to face in operation. This often requires the use of weather parametrization to decrease the grid size. For each point in the conditions grid, the model is used with an optimization algorithm to find the optimal control configuration, resulting in a lookup table that can be used with interpolation for real-time control.

2.4.1 Conditions parametrization

For the 24-hour simulation used in the optimization objective function, the model requires the initial values of T_{zone} and T_{slab} , along with the values of the hourOfDay and the day-OfYear, and hourly values of the following variables: T_{amb} , \dot{Q}_{direct} , $\dot{Q}_{diffuse}$, lux_{SP} , $\dot{Q}_{occEquip}$. Using all of these conditions within the conditions grid would produce a 124-dimensional grid ($4 + 24*5 = 124$), which is significantly more than the 5-7 that is computationally-feasible. To make the grid feasible, some of the variables ($\dot{Q}_{diffuse}$, lux_{SP} , $\dot{Q}_{occEquip}$) are assigned fixed scheduled values over the day: the schedule for $\dot{Q}_{diffuse}$ is derived from average values of the weather file (as shown below), and the schedules for lux_{SP} and $\dot{Q}_{occEquip}$ are derived from the EnergyPlus model. In addition, the hourly values of T_{amb} and \dot{Q}_{direct} are set to be functions of their daily maximum and minimum values, using normalized curves derived from the TMY weather file. These normalized curves are shown for the various climates in the case study descriptions below. For reference, the curves from the Chicago TMY case, along with their daily max and min values over the year, are shown in Figure 12.

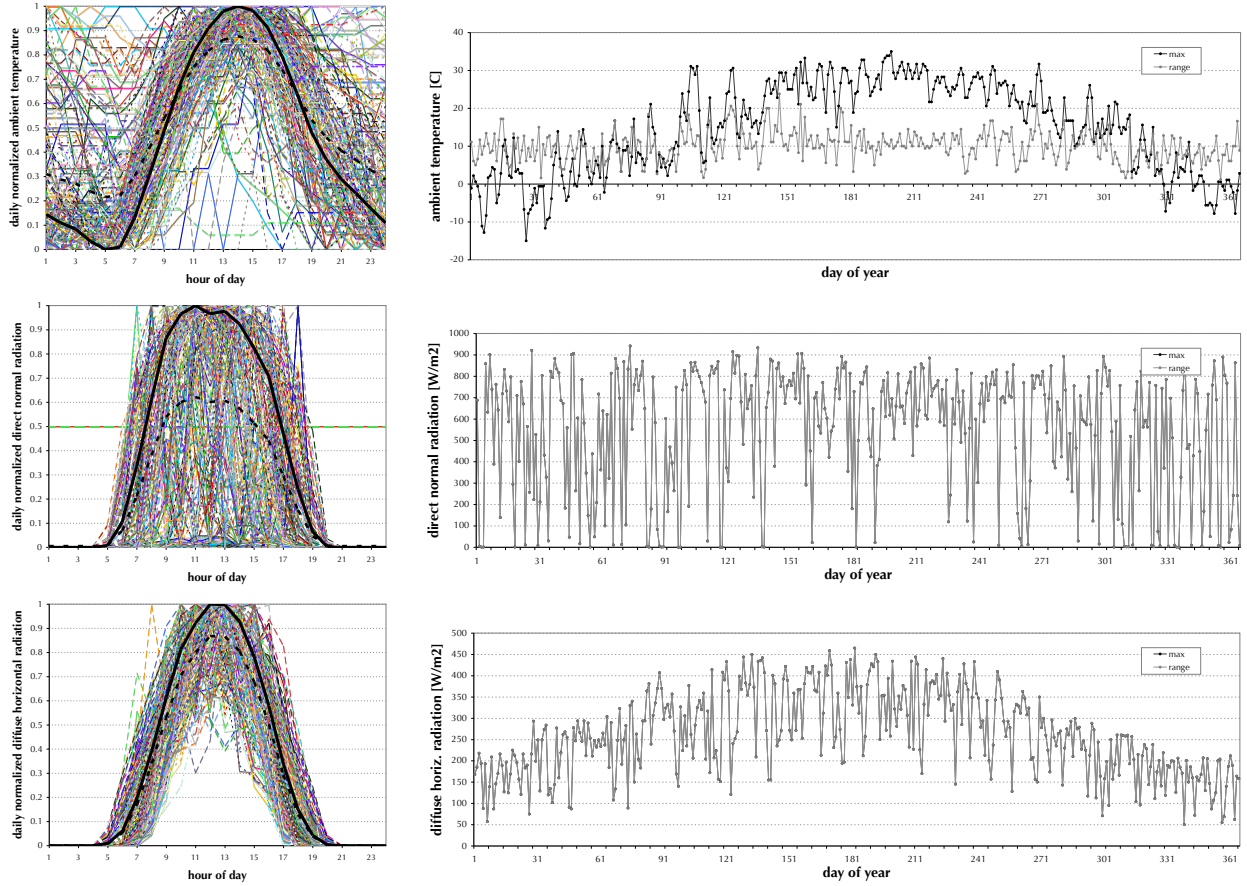
2.4.2 Conditions grid definition and solution

A conditions grid was constructed as shown in Table 2. This 7-dimensional grid has 4860 points which must be optimized. The resulting control lookup tables for each of the cases considered will be shown in the results section below.

Table 2: Conditions grid definition

	min	max	step size
day of year	182	272	90
hour of day	6	21	3
minimum T_{amb}	10	20	5
maximum T_{amb}	20	30	5
maximum \dot{Q}_{direct}	100	800	300
T_{zone0}	19	27	2
T_{slab0}	19	23	2

Figure 12: Conditions parametrizations, Chicago: T_{amb} (top), \dot{Q}_{direct} (middle), and $\dot{Q}_{diffuse}$ (bottom)



2.5 Annual simulations

2.5.1 Configurations

Two different annual simulation configurations were used in this research - the first was temporarily abandoned because of technical difficulties. This first configuration is shown in Figure 13, and uses the Building Control Virtual Test Bed (BCVTB) to link the EnergyPlus model with the controller. In the simulation, the values of the control setpoints (u_{shade} and T_{zoneSP}) are calculated by the controller and fed to EnergyPlus every simulation timestep. BCVTB writes the current state values (T_{zone} and T_{slab}) to a text file before calling the control algorithm via a bat file. The control algorithm also reads in a text file containing the day-ahead predictions of min and max temperatures and max direct and diffuse radiation

2.5.3 Two near-optimal controllers: ‘Lookup’ and ‘luOptCool’

In all of the case studies described below, at least the following two near-optimal controllers are considered: one denoted as ‘lookup’ in the figures and tables, the other denoted as ‘luOptCool’. The ‘lookup’ controller uses the pre-calculated control lookup table with interpolation to determine the control values for both u_{shade} and T_{zoneSP} (over the prediction horizon). This is the way that the control lookup table is generally intended to be used it is simple to implement in annual simulations and would also be simple to implement in physical implementations. However, the 2-level structure of the optimization problem allows for another relatively simple near-optimal controller option: the ‘luOptCool’ controller uses the lookup table with interpolation to determine the control values for just u_{shade} (over the prediction horizon), and then given these value of u_{shade} , an online optimization is performed to determine the control values for T_{zoneSP} . This online optimization is just for the subproblem, and is exactly as described above for the subproblem linear programming optimization using the Simplex algorithm, which takes just a matter of seconds to run. The ‘luOptCool’ controller may thus be thought of as a hybrid controller, part of it using a pre-calculated offline-optimization lookup table, and part of it using online optimization. Instead of using only the daily minimum and maximum values of temperature and radiation, this controller uses the hourly day-ahead predicted values. It performs better than the ‘lookup’ controller because it avoids the performance penalties associated with both conditions parametrization and lookup interpolation for the cooling optimization variables (but it still has these performance penalties for the shading optimization variables, so it performs somewhat less well than would a full online MPC configuration).

2.5.4 Control block length in case studies

In the case studies below, the control lookup tables were computed for varying hourOfDay values (with the exception of the internal Venetian blind and electrochromic cases, because of dwindling computation time availability), but the annual study results presented below are only for the case with a control block length of 24 hours - ie. only for the case where at midnight the controller determines the setpoints for the entire upcoming day and all of them are implemented and controller is not called upon again until the following midnight. The cases with shorter block lengths, e.g. 4 hours, where the controller determines the values for the full day ahead but only the first 4 hours get implemented before the controller is called upon again to determine the values for the day ahead again from this new starting point - although these shorter block length cases should have shown slightly better performance than the 24-hour block length cases, they actually performed slightly worse. Further investigations are required to determine why this happened. However, because the annual simulations are using perfect day-ahead predictions and zero model mismatch (ie. the annual simulation model and the controller model are identical), the performance gains with a shorter block length should be small; the 24-hour block length results are good indicators of the energy savings potential.

3 Simulation studies of savings potential: Case descriptions

3.1 Overview: Case study configurations

The purpose of these simulation studies is both to test the methods described above and to estimate the energy savings potential available from integrated near-optimal control of some common operable shading technologies and massive-slab radiant cooling. As such, three different operable shading technologies are considered, and they are applied in four different climates, and two different orientations. The three operable shading technologies are (1) external Venetian blinds, (2) internal Venetian blinds, and (3) electrochromic windows. The four climates being considered are (a) Chicago, (b) Houston, (c) New York and (d) Sacramento. The two orientations are (S) South and (W) West. For the South orientation, all twelve (3x4) combinations of shading technologies and climates are considered. For the West orientation, all four climates are considered but only one shading technology (external Venetian blinds). So a total of 16 case studies are considered.

In each case study, the three base case heuristic control strategies are applied as described in the previous section. At least two varieties of near-optimal control are also applied in each case, also as described above: ‘lookup’, with both the shading and cooling setpoints determined by interpolation of a pre-computed lookup table; and ‘luOptCool’ with the shading setpoints determined by lookup table interpolation and the cooling setpoints determined by online optimization (fast, since it is just a simplex algorithm), given the shading setpoints. The cases with South-facing external Venetian blinds were studied in greater detail than the other case, and results are shown in those cases for different lookup tables and other near-optimal control variants to more thoroughly describe the nature of the control challenge and how the controllers are working.

In the results section below, the 16 case studies are organized into four groups: (1) external Venetian blinds, South zone; (2) external Venetian blind, West zone; (3) internal Venetian blind, South zone; and (4) electrochromic window, South zone.

Offline-optimization lookup tables were not constructed for all of the 16 cases, but rather just for the Chicago cases, and then applied to the other climates. Thus for the non-Chicago climates the lookup tables used for their near-optimal control are not perfectly matched. However, as described below, their differences in construction are small, and the Chicago-based lookup tables do provide a reasonably good approximation to what the lookup tables would be for the other climates if they had been calculated out in full: an extra Houston-based lookup table was constructed for the external Venetian blind - South zone case and applied to all four climates to investigate how the different lookup table basis affects the near-optimal control performance.

Section 3.2 describes the details of the three shading technology configurations considered. Section 3.3 then shows the reduced-order model configuration for the 16 cases, in particular describing their shading grids (f_1 in the model equations) and thermal model parameters (which are independent of shading technology or climate, and change only with

orientation because of the corresponding differences in zone sizes). Section 3.4 then describes the additional configuration information used in calculating the lookup tables - in particular, the conditions parametrization curves that are a function of the climate.

3.2 Fenestration system descriptions

The case studies are all based on the modified ASHRAE 90.1-2010 model described in the methods section above, with just the fenestration systems changing between the three configurations: external Venetian blinds, internal Venetian blinds, and electrochromic windows. Their descriptions within EnergyPlus are shown below.

3.2.1 Venetian blinds

The Venetian blinds material description is the same in both the external and internal cases, and is shown in Table 3. It was based on an example file from the EnergyPlus standard download. The associated windows in both cases are the same as those used in the ASHRAE 90.1-2010 model: double-paned glazing with window properties of SHGC=0.40, Tvis=0.52, U-value=2.95 W/m²-K. The effects of the blind position and blind state on solar gains and daylighting is shown in the shading grid graphs below.

3.2.2 Electrochromic windows

The electrochromic window descriptions start from the given double-paned glazing description, but with the external pane replaced with an electrochromic glass. Two glass states are described - clear and tinted - and the state is controlled with a scheduled value between 0 (clear) and 1 (tinted). The two states' outside glass layer descriptions use detailed spectral data sets with resultant window properties of SHGC=0.43-0.13, Tvis=0.50-0.01, U-value=2.88 W/m²-K. The effects of the two glass states on solar gains and daylighting is shown in the shading grid graphs below.

Table 3: Venetian blinds material description (WindowMaterial:Blind in EnergyPlus)

<i>Property</i>	<i>Value</i>
Slat orientation	Horizontal
Slat width (m)	0.025
Slat separation (m)	0.01875
Slat thickness (m)	0.001
Slat angle (deg)	90
Slat conductivity (W/m.K)	44.9
Slat beam solar transmittance	0
Front Side Slat beam solar reflectance	0.8
Back Side Slat beam solar reflectance	0.8
Slat diffuse solar transmittance	0
Front Side Slat diffuse solar reflectance	0.8
Back Side Slat diffuse solar reflectance	0.8
Slat beam visible transmittance	0
Front Side Slat beam visible reflectance	0.8
Back Side Slat beam visible reflectance	0.8
Slat diffuse visible transmittance	0
Front Side Slat diffuse visible reflectance	0.8
Back Side Slat diffuse visible reflectance	0.8
Slat Infrared hemispherical transmittance	0
Front Side Slat Infrared hemispherical emissivity	0.9
Back Side Slat Infrared hemispherical emissivity	0.9
Blind-to-glass distance (m)	0.05
Blind top opening multiplier	0
Blind bottom opening multiplier	0
Blind left-side opening multiplier	0.5
Blind right-side opening multiplier	0.5

3.3 Reduced-order model descriptions

Between the various simulation cases, only two aspects of the reduced-order model change: the shading grid (f_1 in the model equations), and the parameters associated with the thermal parts of the model (UA_{zone} , h_c , $c_{zoneCap}$ and $c_{slabCap}$).

3.3.1 Shading grids

As noted in Equation 1, the influence of the fenestration system on the solar gains and daylighting is included within the reduced-order model as follows.

$$[\dot{Q}_{solZone}, \dot{Q}_{solSlab}, lux_{DL}] = f_1(u_{shade}, \text{day}, \text{hr}, \dot{Q}_{direct}, \dot{Q}_{diffuse})$$

For each of the 16 simulation case studies, a lookup table was produced for this function f_1 , called a ‘shading grid’ herein. The lookup tables were produced by running batches of EnergyPlus simulations and post-processing the results, as described in the methods

section above. The lookup tables are 5-dimensional, and thus difficult to visualize. They are stored in simple csv text files, each line representing a 5-dimensional point, sorted in ascending order first by u_{shade} , then by \dot{Q}_{direct} , then by $\dot{Q}_{diffuse}$, then by day of year and by hour of day. In the graphs below, the horizontal axis is simply the line number of the csv text file. So for the Venetian blind cases, there are five visible groups from left to right corresponding to the five possible blind positions, and within each group the values of \dot{Q}_{direct} and $\dot{Q}_{diffuse}$ are increasing from left to right. For the electrochromic cases, there are only two possible shading states within the EnergyPlus model, so there are only two major groups in those graphs.

Note how the interior Venetian blinds (Figure 16) show much higher zone solar gains when the blinds are closed (in positions of 0° or 180°) than do the exterior Venetian blinds (Figures 14 and 15). Also note that in the Venetian blinds cases the floor solar gains are highest when the blinds are rotated slightly upwards to 135° . The electrochromic windows produce much more daylight in their clear state than do either of the Venetian blind configurations (since the Venetian blinds are being modeled as always deployed, with just the blind angle changing), and that the darkened state effectively eliminates daylighting and floor solar gains but still produces some zone solar gains.

Also note that given a particular fenestration system, the only thing changing between climates that can affect the shading grid is the latitude.

3.3.2 Thermal parameters

The thermal parameter values used in the case studies are shown in Table 4. The values of the South zone were produced through calibration against the EnergyPlus model as described in the calibration section above. To save computation time, the values used for the West zone were simply scaled from those in the South zone, based on the differences in floor area.

Table 4: Calibrated parameter values for the thermal aspects of the model

South zone		West zone	
parameter	value	parameter	value
UA_{zone}	320	UA_{zone}	213.3
h_c	2600	h_c	1733.3
$c_{zoneCap}$	4000	$c_{zoneCap}$	2666.7
$c_{slabCap}$	14000	$c_{slabCap}$	9333.3

Note that by keeping the thermal parameters the same in the different climates, we are considering the case where the exact same building (including the same wall construction) is being simulated in different climates. In future iterations of this research, if they are to occur, one may wish to consider different constructions in different climates - in that case, the thermal calibration would have to be repeated for each different building description (ie. for each different climate).

Figure 14: Shading grids: Exterior Venetian blinds, South-facing

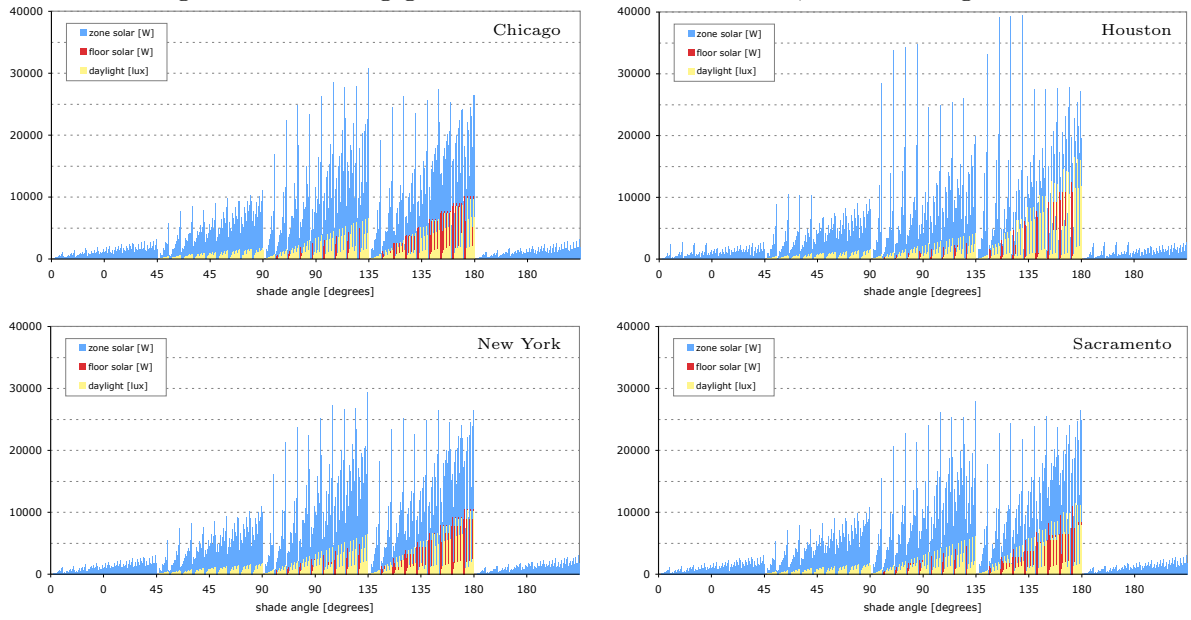


Figure 15: Shading grids: Exterior Venetian blinds, West-facing

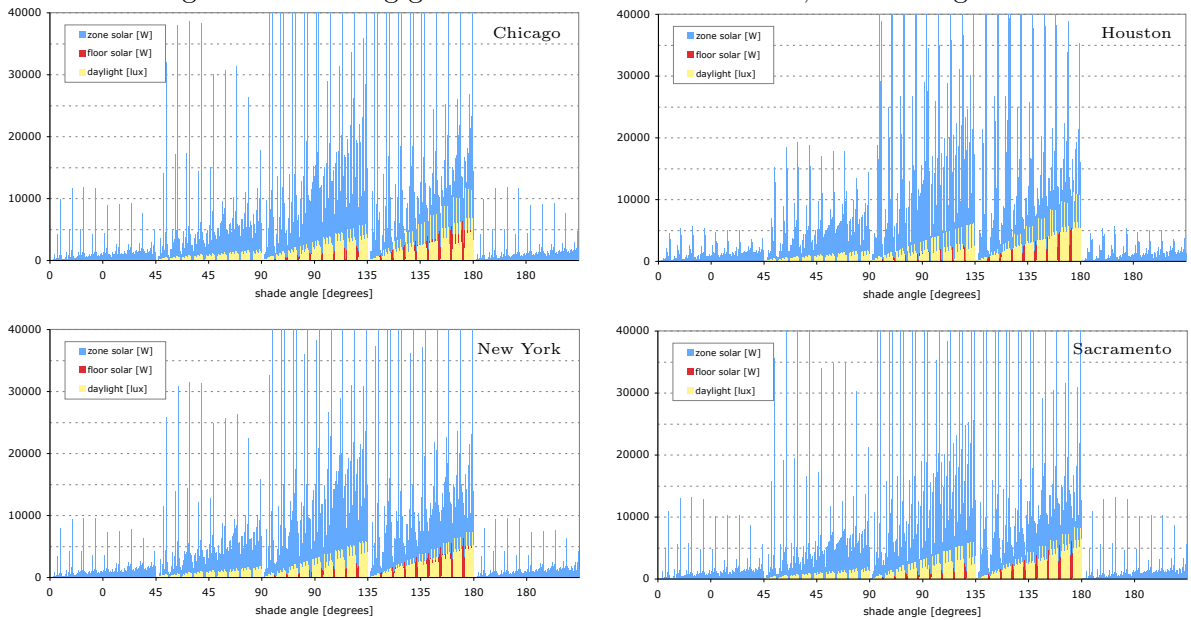


Figure 16: Shading grids: Interior Venetian blinds, South-facing

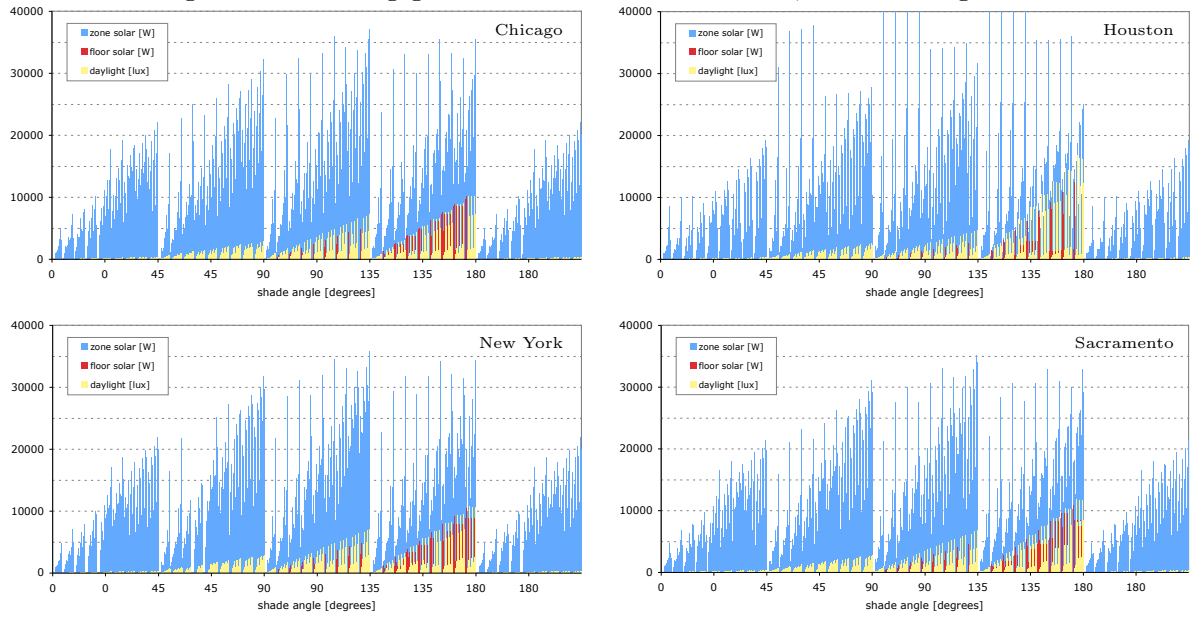
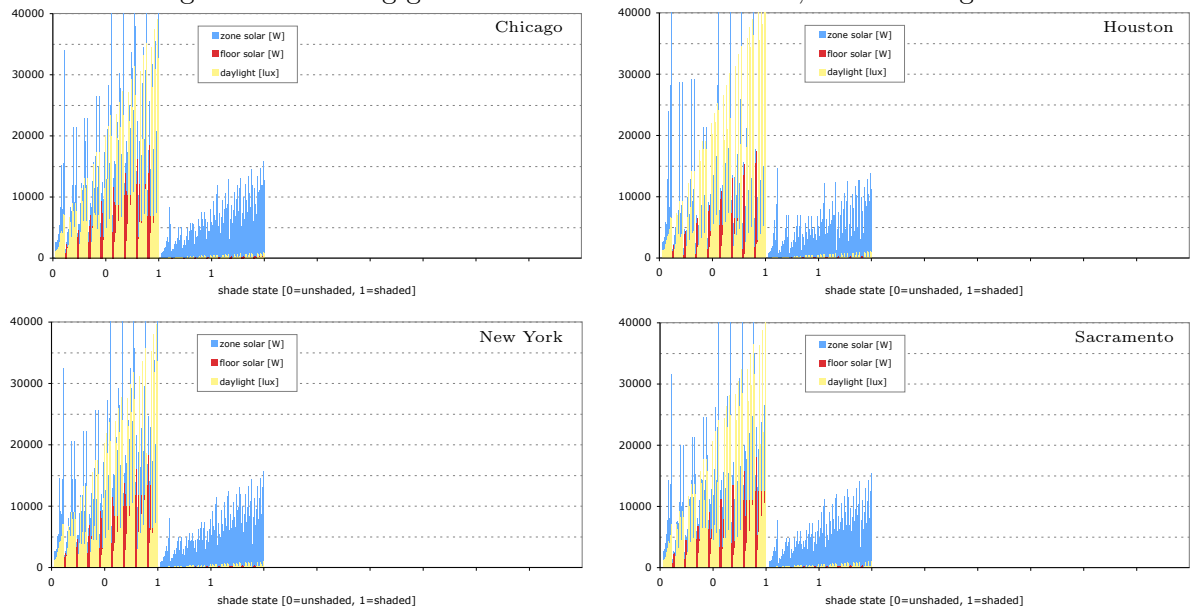


Figure 17: Shading grids: Electrochromic windows, South-facing



3.3.3 Schedules of internal loads and lighting setpoints

The daily schedules for the internal loads ($\dot{Q}_{occEquip}$) and lighting setpoints (lux_{SP}) are shown in Table 5. These are used in the annual simulations and in the control lookup table calculations. These values were derived from the EnergyPlus model.

Table 5: Internal loads schedule and lighting setpoint schedule

hours	1-5	6-7	8-11	12	13-16	17-21	22	23-24
QoccEquip	754	754	4077	2927	4077	1159	1159	754
luxSP	23	500	500	500	500	98	23	23

3.4 Lookup table calculation configurations

As noted above, five offline-optimization control lookup tables were produced: one for each of the three fenestration systems options for the South zone in Chicago, one for the West zone with external Venetian blinds in Chicago, and one for the South zone with external Venetian blinds in Houston. In each case, the conditions grid and optimization configuration were the same as described in the methods section above. The 4860 GenOpt optimizations required for each case were carried out on either Amazon EC2 linux machines (in the case of Chicago-South-externalVenetian) or on the Lawrencium cluster at LBNL (for the rest of the cases): these computations required about 1500 processor-hours on the Amazon cloud (roughly \$150) or about 600 processor-hours on the Lawrencium cluster. (Note that previous iterations of these studies, using GenOpt for both the shading and the cooling, instead of using the two-level optimization configuration, required a great deal more computing - approximately 5000 processor-hours for one case.)

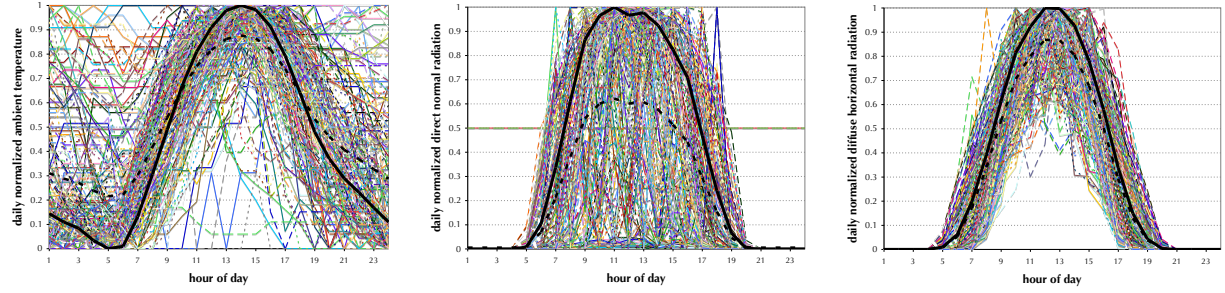
What changes between the five control lookup table calculation configurations is the reduced-order model being used within the objective function (ie. the shading grid and thermal parameters for the case being considered), and the conditions parametrization curves that are dependent on the climate - these are the curves that are used to translate from the daily min and max values of T_{ambMax} , T_{ambMin} and $\dot{Q}_{directMax}$ (and the constant $\dot{Q}_{diffuseMax} = 200$) used in the conditions grid to the hourly values of T_{amb} , \dot{Q}_{direct} and $\dot{Q}_{diffuse}$ used in the model.

3.4.1 Conditions parametrization for lookup tables

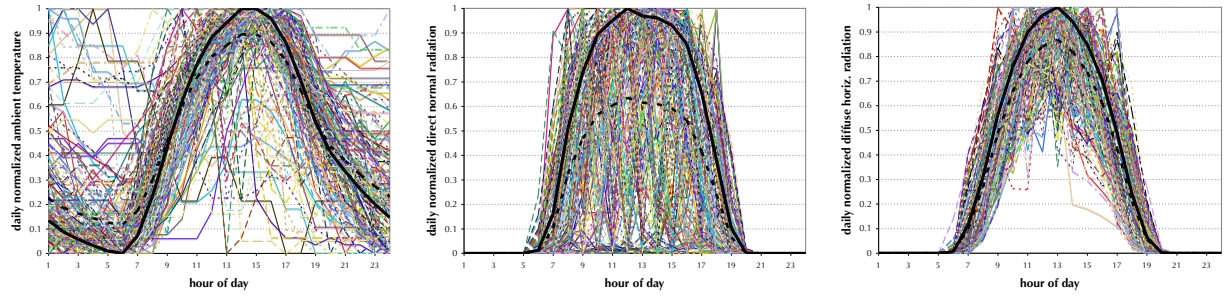
Most of the lookup tables were constructed based on the Chicago case, and thus use the conditions parametrization curves shown in Figure 18a. However, one of the lookup tables uses the Houston case, and thus uses the conditions parametrization curves shown in Figure 18b. Figure 18c and 18d, for New York and Sacramento, are included here to show how similar these curves are for different climates.

Figure 18: Conditions parametrizations curves

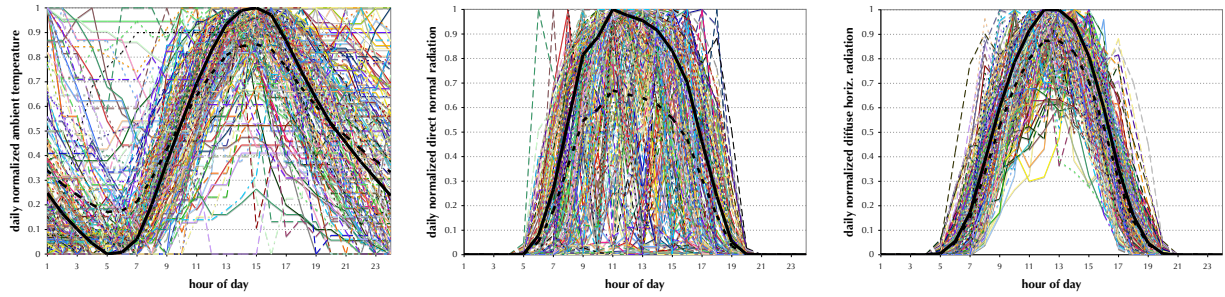
(a) Chicago



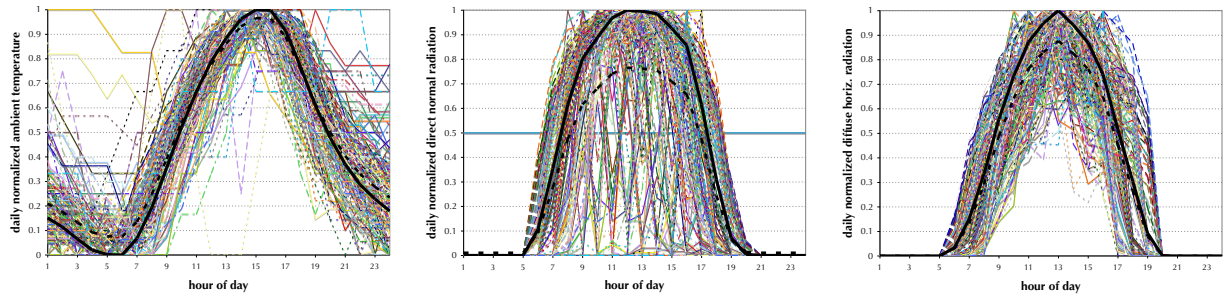
(b) Houston



(c) New York



(d) Sacramento



4 Simulation studies of savings potential: Results

The annual results of the 16 case studies are presented below, grouped by their fenestration technology and orientation. The hourly simulation outputs, along with their monthly and annual summaries, can be reviewed in detail in the Excel files located here:

<https://s3.amazonaws.com/facadeHVACcontrolOpt/annualResultsExternalVenetianSouth.zip>

<https://s3.amazonaws.com/facadeHVACcontrolOpt/annualResultsExternalVenetianWest.zip>

<https://s3.amazonaws.com/facadeHVACcontrolOpt/annualResultsInternalVenetianSouth.zip>

<https://s3.amazonaws.com/facadeHVACcontrolOpt/annualResultsElectrochromicSouth.zip>

These Excel files allow the reader to compare the control strategies in as much detail as they wish. In this section, we show some of the details of the external Venetian blinds South zone case, but otherwise focus on the annual summaries. In general, the external Venetian blinds South zone case is used as the illustrative case in the discussion herein, and is described in much greater detail below than are the remaining cases.

Regardless of whether the reader wishes to download and dig into the annual simulation results details, it is strongly recommended that the control lookup tables are downloaded from the following link and explored with their Excel graphing tools:

<https://s3.amazonaws.com/facadeHVACcontrolOpt/controlLookupTables.zip>

One of the most useful aspects of the lookup table approach to approximating MPC is that the control responses can be readily explored through simple interfaces such as those in the download. The user can select the values of the conditions variables by using the pull-down menus at the top of the page, and the optimal control responses over the prediction horizon are automatically graphed below.

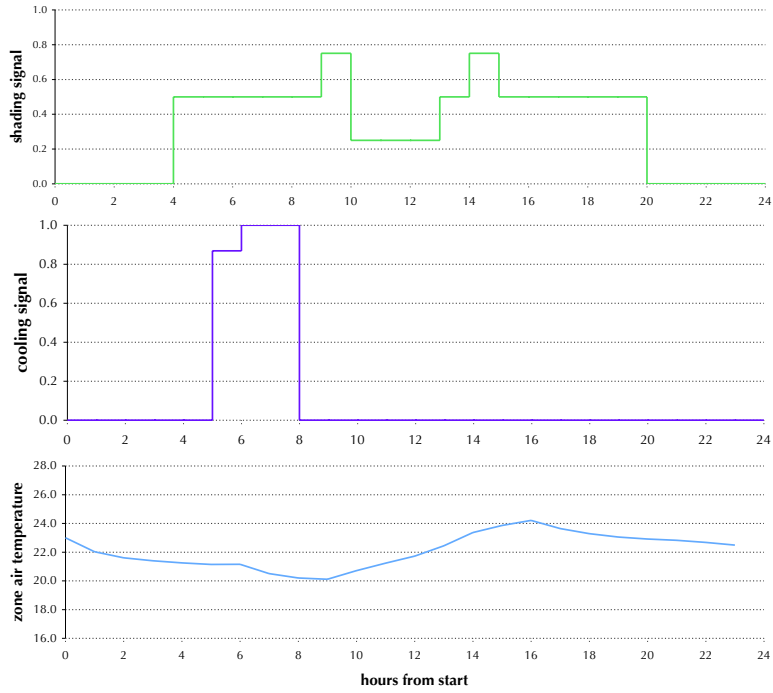
4.1 External Venetian blinds, South zone

4.1.1 Control lookup tables

For this case of external Venetian blinds, South zone, two different control lookup tables were constructed: one based on the Chicago case (ie. using the Chicago conditions parametrization curves and the Chicago shade grid), and the other based on the Houston case. Figure 19 shows two example responses from the control lookup table based on the Chicago case. Note how the cooling profile changes with a different diurnal temperature range: with a larger range it cools earlier in the morning, since there is more of an advantage to earlier pre-cooling because of the COP differences; but with a smaller range it cools somewhat later, balancing the pre-cooling COP benefit against the penalty of increased thermal gains associated with pre-cooling (because of the increased indoor-outdoor temperature difference and thus heat gain through the envelope).

Figure 19: Examples from control lookup table, external Venetian blinds, South, Chicago

$\{ T_{ambMax} = 30, T_{ambMin} = 15, \dot{Q}_{directMax} = 500, \text{dayOfYear} = 182, \text{hourOfDay} = 1, T_{zone0} = 23, T_{slab0} = 21 \}$



$\{ T_{ambMax} = 30, T_{ambMin} = 20, \dot{Q}_{directMax} = 500, \text{dayOfYear} = 182, \text{hourOfDay} = 1, T_{zone0} = 23, T_{slab0} = 21 \}$

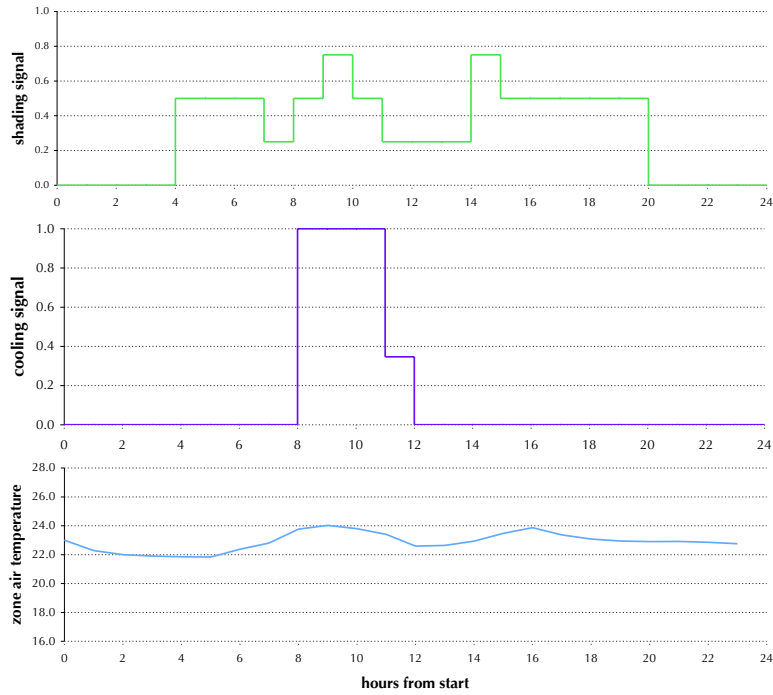
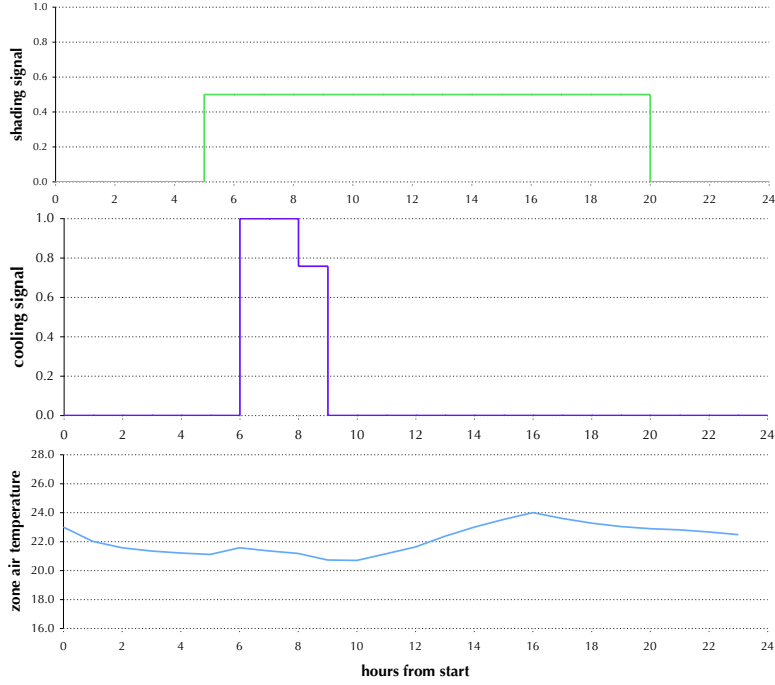
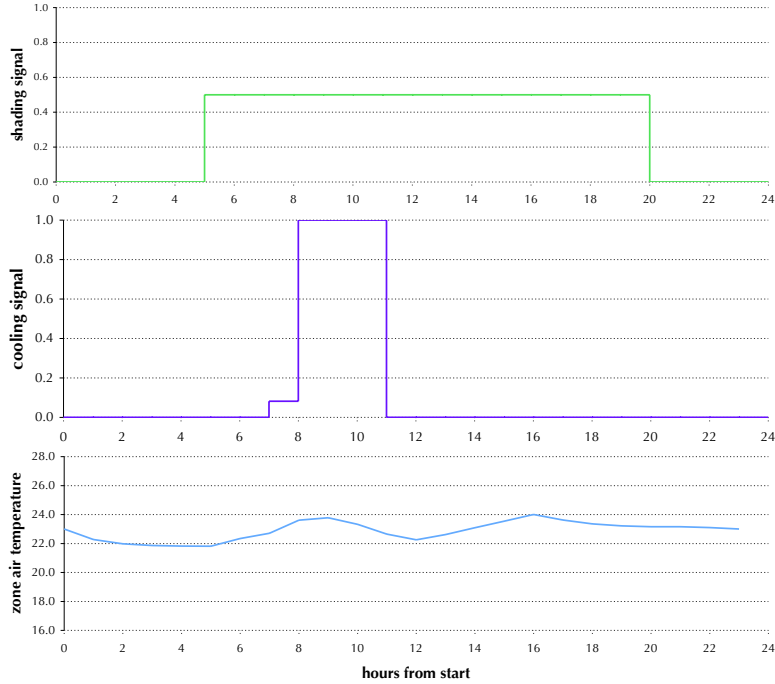


Figure 20: Examples from control lookup table, external Venetian blinds, South, Houston

$\{ T_{ambMax} = 30, T_{ambMin} = 15, \dot{Q}_{directMax} = 500, \text{dayOfYear} = 182, \text{hourOfDay} = 1, T_{zone0} = 23, T_{slab0} = 21 \}$



$\{ T_{ambMax} = 30, T_{ambMin} = 20, \dot{Q}_{directMax} = 500, \text{dayOfYear} = 182, \text{hourOfDay} = 1, T_{zone0} = 23, T_{slab0} = 21 \}$



4.1.2 Annual simulation details, Chicago case

Annual simulations were run for five different control strategies: the three base cases described in the methods section (Base1 = shading position kept at 90° , zone temp setpoint always 24C; Base2 = shading position kept at 0° , zone temp setpoint always 24C; Base3 = a heuristic pre-cooling strategy with afternoon shade closing); a case using interpolation of the control lookup table for both the shading setpoint and the zone temperature setpoint; and a case using interpolation of the control lookup table for the shading input and performing an online optimization for the zone temperature setpoints. The behavior of these five control strategies can be seen in Figure 22 for the period of July 1 to July 7. Monthly summaries of the heating, cooling and lighting energy use are shown in Figure 21, where ‘lookup’ refers to the use of the control lookup table for both shading and cooling, and ‘luOptCool’ to the use of the lookup table for shading and online optimization for cooling.

Figure 21: External Venetian blinds, South zone, Chicago, monthly results

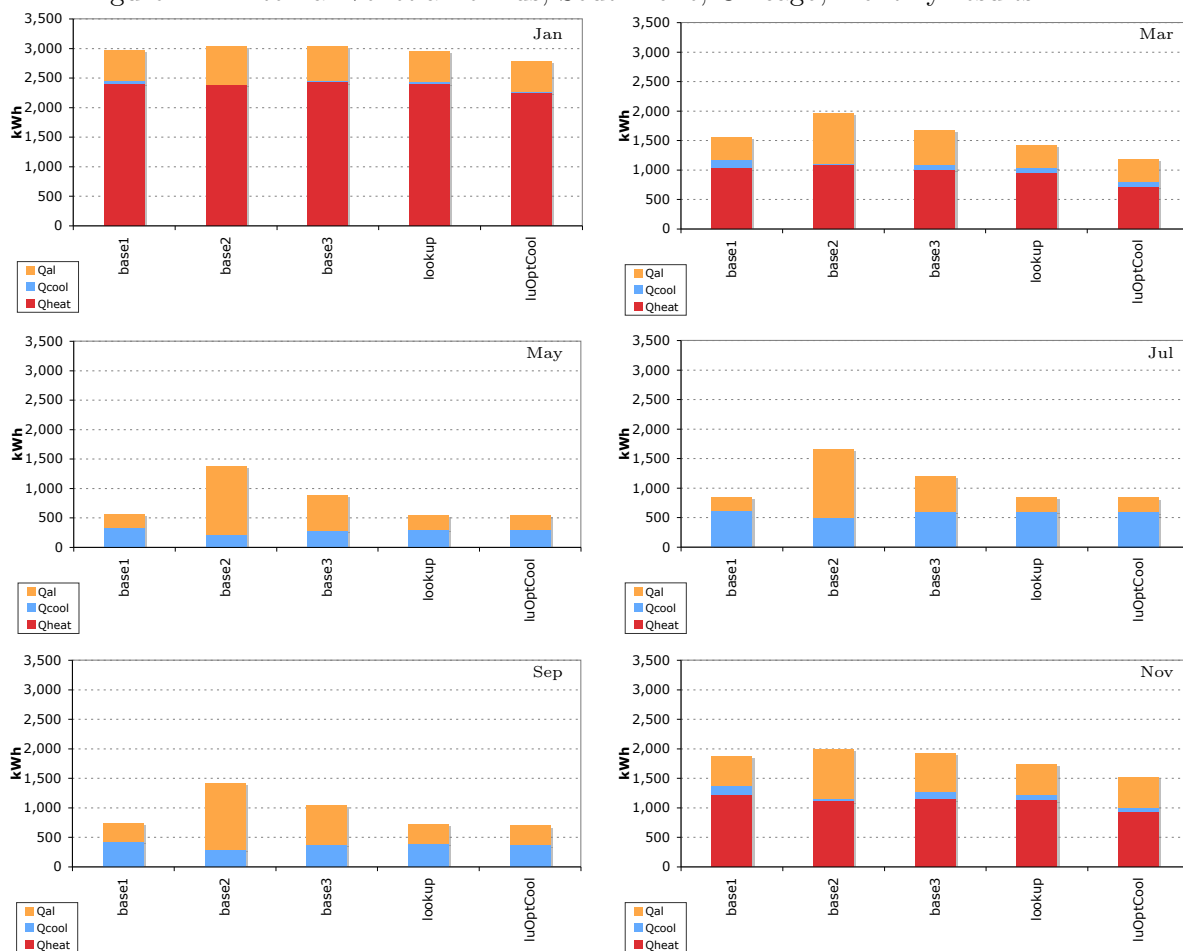
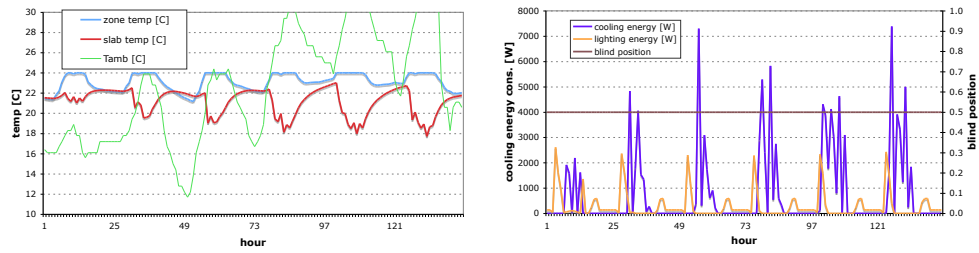
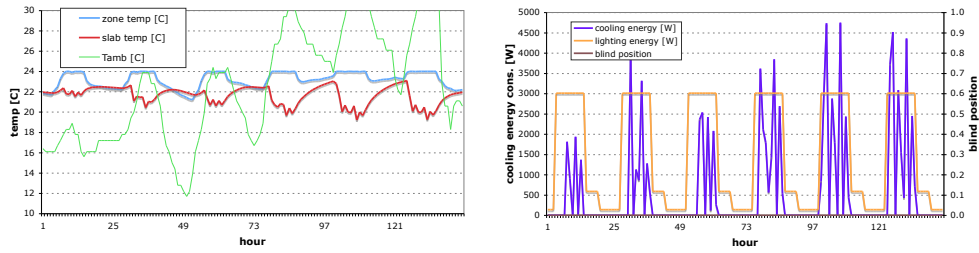


Figure 22: External Venetian blinds, South zone, Chicago, July 1-7 Details

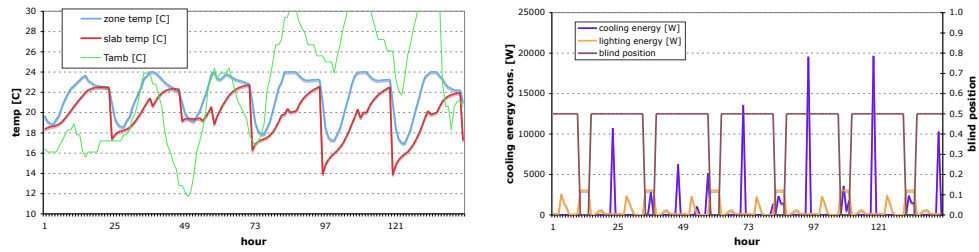
Base1: shading position kept at 90°, zone temp setpoint always 24C



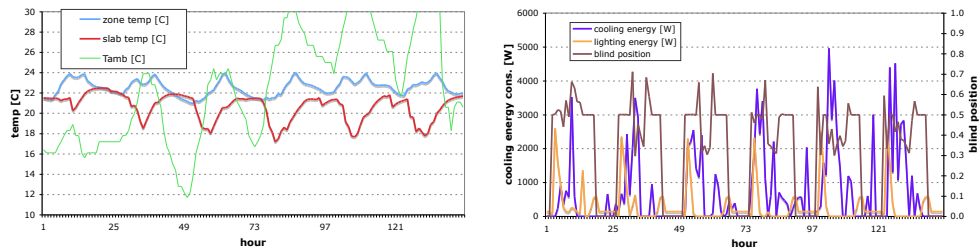
Base2: shading position kept at 0°, zone temp setpoint always 24C



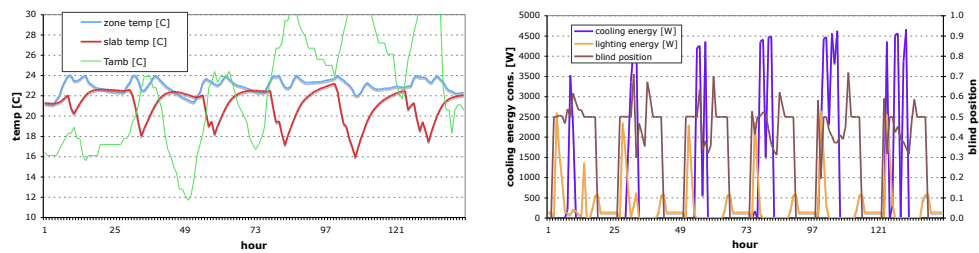
Base3: a heuristic pre-cooling strategy with afternoon shade closing



Lookup table control of both shading and cooling



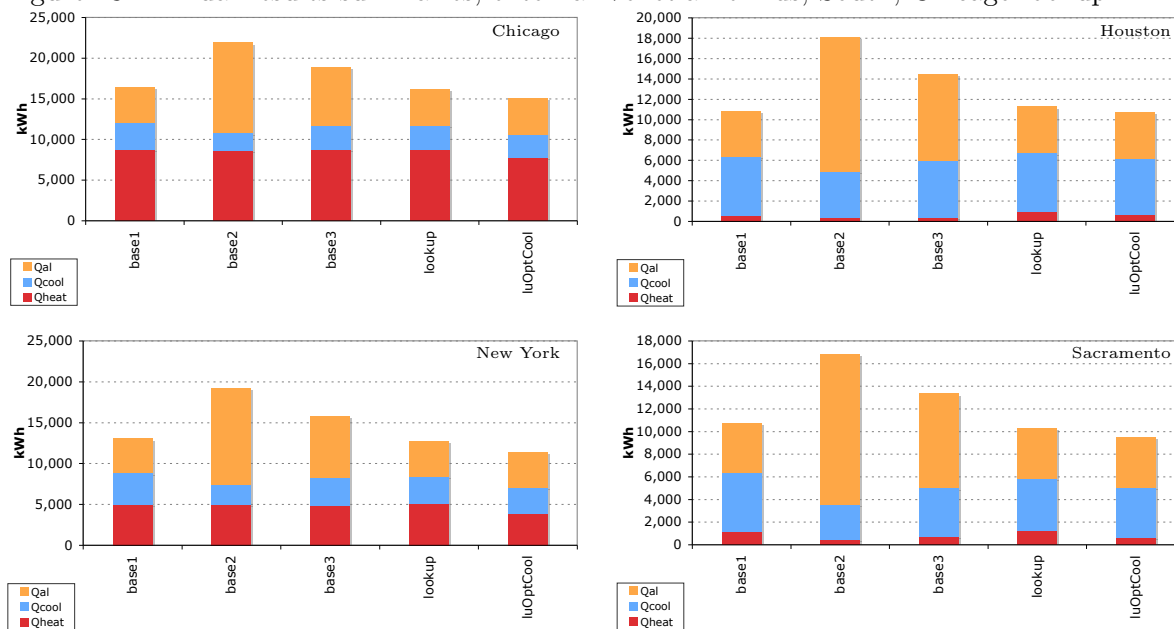
Lookup table control of shading with online optimization of cooling



4.1.3 Annual simulation results, all climates

Figure 23 shows the annual energy consumption results for all four climates considered, using the Chicago-based lookup table for all four cases. We will generally disregard the heating energy in our discussion - the optimization-based controllers were not designed with heating in mind, and their effects on heating (relative to Base1) tend to be small, unintended, and generally in favor of the optimization-based controllers. Note that Base1 significantly outperforms Base2 and Base3 in all of the climates, and that the two optimization-based controllers tend not to perform much better than Base1.

Figure 23: Annual results summaries, external Venetian blinds, South, Chicago lookup



The relative performance of the three base cases sheds some light on the nature of the control challenge for this particular building configuration. Base1 represents the case where the shades are generally letting in nearly as much light and solar gains as possible, and thus uses nearly the minimum possible amount of lighting energy but more cooling energy than the other cases might. Base2 represents the case where the blinds are closed all the time, thus minimizing the cooling requirement (although not necessarily the cooling energy since it does not do any active pre-cooling to take advantage of COP differences with outdoor temperature), but maximizing the lighting energy. The annual energy differences between Base1 and Base2 demonstrates how the lighting penalty associated with closing the blinds is usually much more significant than the cooling savings it brings. Base3 generally keeps the blinds open most of the day except a few hours in the afternoon, but

note how much of a lighting penalty it takes relative to Base1 for a relatively small benefit in cooling energy. The optimization-based control lookup table (Figure 19 above) thus tends to keep the blinds open (horizontal, 90°) for most of the day, closing them only partially at select times, usually around noon or the early afternoon - the resulting lighting energy thus tends to be slightly higher in the optimization-based cases than in Base1. The cooling savings relative to Base1 come from these minor but timely decreases in solar gains working together with the active pre-cooling of the slab to take advantage of the lower cooling COP earlier in the day. The optimization must thus make a complex trade-off between the increase in lighting energy and the decrease in cooling energy. Note also that the decrease in cooling energy because of the lower COP is slight, since the COP sensitivity to ambient temperature (based on the EnergyPlus model) is slight. Base3 shows that this shading trade-off and the pre-cooling benefit is tricky - using a simple heuristic like in this case can easily increase the annual energy consumption relative to the very simple Base1.

Figure 24 compares the annual cooling + lighting energy for Base1 and the two optimization-based controllers. The lookup table controller generally performs slightly better than Base1 but only by a few percent. Using online optimization for the cooling control, which is quick to do online because of it being an analytic optimization, eliminates the performance losses associated with the lookup interpolation for the cooling, and produces savings that are a few percent higher. Note that the lookup table performs poorly in Houston, which may be because the lookup table was based on Chicago which has a significantly different latitude (and thus a significantly different shading grid, unlike the other two cases). The details of the cooling and lighting savings are shown in Table 6.

Figure 24: Comparisons of annual results, external Venetian blinds, South, Chicago lookup

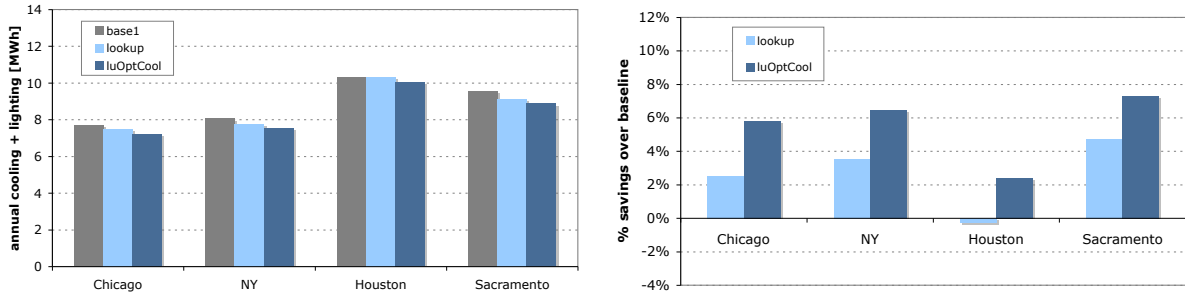


Table 6: Percent savings relative to Base1, external Venetian blinds, South, Chicago lookup

	Chicago			NY			Houston			Sacramento		
	light	cool	total	light	cool	total	light	cool	total	light	cool	total
lookup	-2.4	9.2	2.6	-2.3	10.0	3.5	-3.9	2.5	-0.3	-2.0	10.4	4.7
luOptCool	-2.3	16.5	5.8	-2.1	16.0	6.5	-3.7	7.0	2.4	-2.0	15.2	7.3

Figures 25 and 26 and Table 7 show the results for the same set of annual simulations, but this time using the Houston-based control lookup table instead of the Chicago-based one. The results suggest that there might be something wrong with the Houston-based control lookup table. Further analysis is required to determine why this might be the case.

Figure 25: Annual results summaries, external Venetian blinds, South, Houston lookup

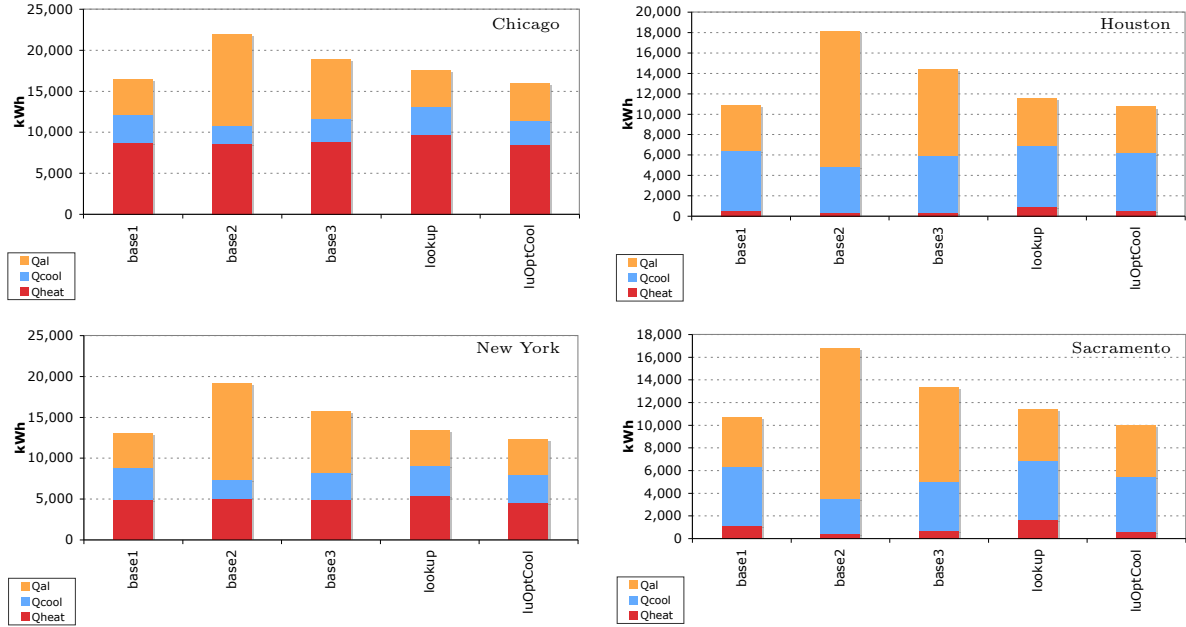


Figure 26: Comparisons of annual results, external Venetian blinds, South, Houston lookup

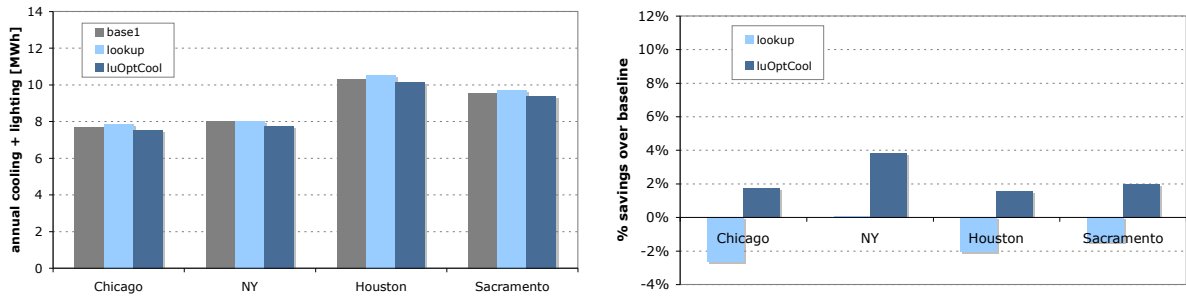


Table 7: Percent savings relative to Base1, external Venetian blinds, South, Houston lookup

	Chicago			NY			Houston			Sacramento		
	light	cool	total	light	cool	total	light	cool	total	light	cool	total
lookup	-2.9	-2.3	-2.6	-3.1	3.7	0.1	-3.8	-0.7	-2.0	-3.1	0.0	-1.4
luOptCool	-3.0	8.0	1.7	-3.2	11.7	3.8	-2.5	4.6	1.6	-2.8	6.0	2.0

4.2 External venetian blinds, West zone

4.2.1 Control lookup table

Figure 29 shows two example points in the control lookup table (the same two sets of conditions used in the previous lookup table graphs). Note that the control responses are broadly similar to those calculated for the South zone for these conditions, but with somewhat more cooling required in the West case and it is applied somewhat later in the day, and with slightly more shading movement away from the 90° position in the afternoon.

4.2.2 Annual simulation results

The annual simulation results are summarized in Figures 27 and 28, and in Table 8. They show less energy savings than were found for the South zone cases.

Figure 27: Annual results summaries, external Venetian blinds, West, Chicago lookup

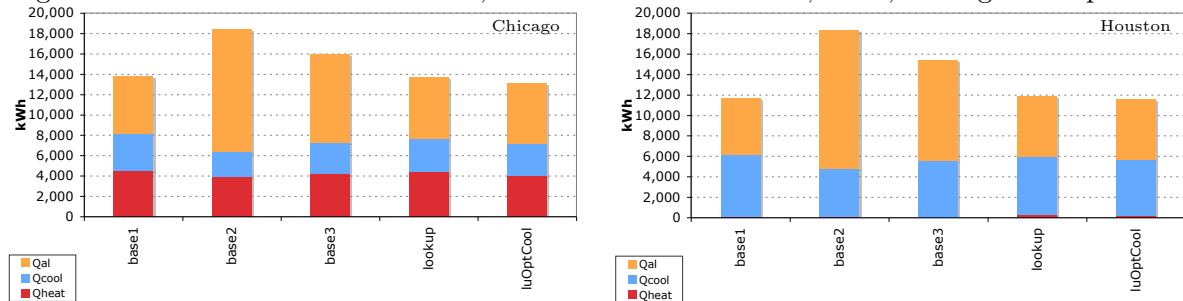


Figure 28: Comparisons of annual results, external Venetian blinds, West, Chicago lookup

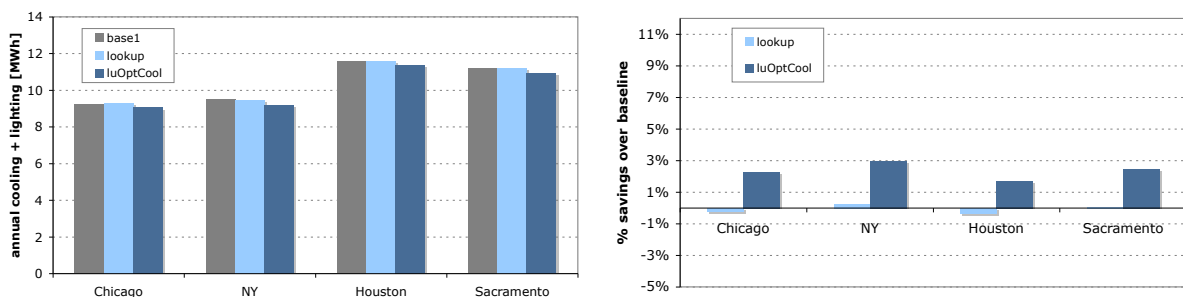
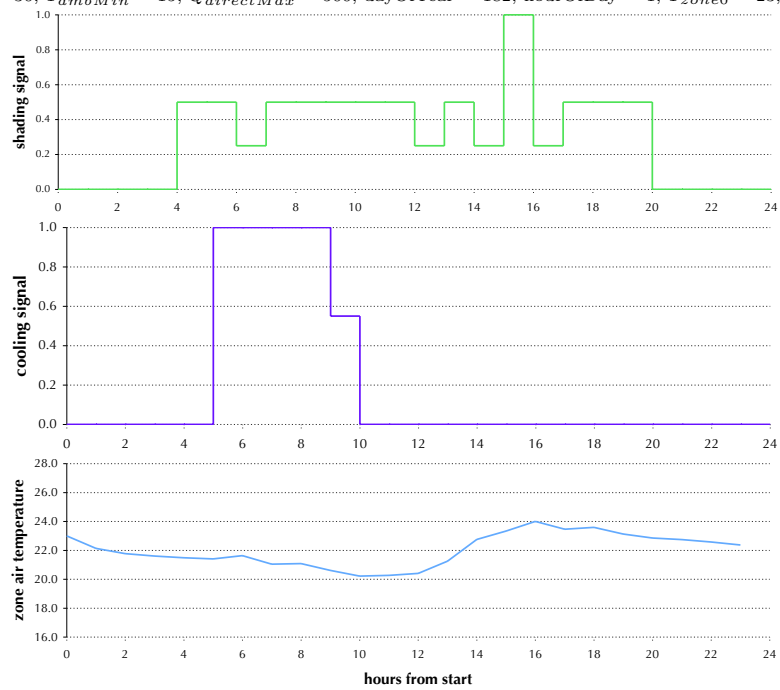


Table 8: Percent savings relative to Base1, external Venetian blinds, West, Chicago lookup

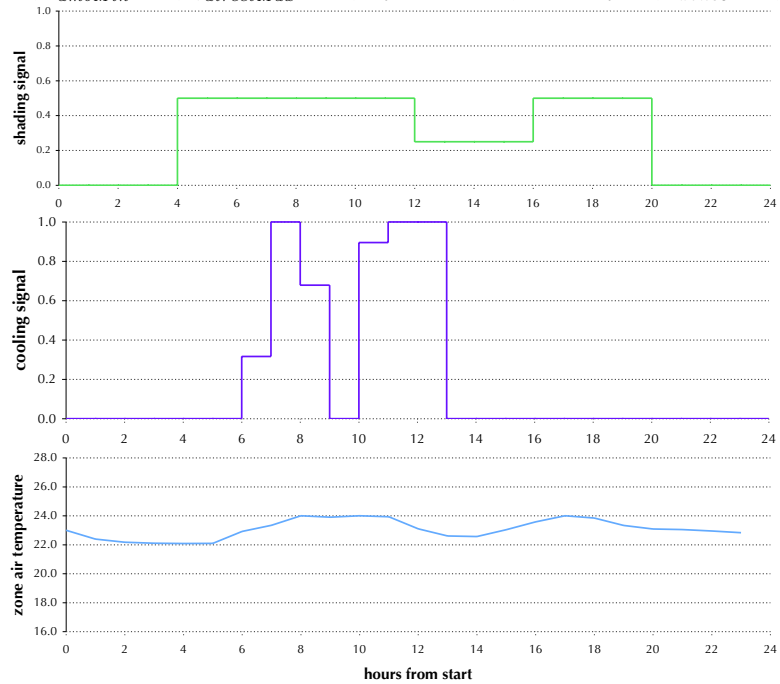
	Chicago			NY			Houston			Sacramento		
	light	cool	total	light	cool	total	light	cool	total	light	cool	total
lookup	-5.3	7.9	-0.2	-5.1	7.9	0.3	-7.7	6.4	-0.3	-12.5	12.5	0.1
luOptCool	-4.4	12.9	2.3	-4.3	13.4	3.0	-6.1	8.9	1.7	-9.6	14.5	2.5

Figure 29: Examples from control lookup table, external Venetian blinds, West, Chicago

$\{ T_{ambMax} = 30, T_{ambMin} = 15, \dot{Q}_{directMax} = 500, \text{dayOfYear} = 182, \text{hourOfDay} = 1, T_{zone0} = 23, T_{slab0} = 21 \}$



$\{ T_{ambMax} = 30, T_{ambMin} = 20, \dot{Q}_{directMax} = 500, \text{dayOfYear} = 182, \text{hourOfDay} = 1, T_{zone0} = 23, T_{slab0} = 21 \}$



4.3 Internal venetian blinds, South zone

4.3.1 Control lookup table

Figure 32 shows two example points in the control lookup table. The control signals are similar to those of the external Venetian blinds, except that more cooling is required.

4.3.2 Annual simulation results

The annual simulation results are summarized in Figures 30 and 31, and in Table 9. The energy savings are quite small. The blind position has less impact on the cooling load in the internal Venetian blind case than it does in the exterior Venetian blind case, so there is less possibility for cooling energy savings - this is reflected in the lower savings for annual cooling here (Table 9) than in the external Venetian blind case (Table 6).

Figure 30: Annual results summaries, internal Venetian blinds, South, Chicago lookup

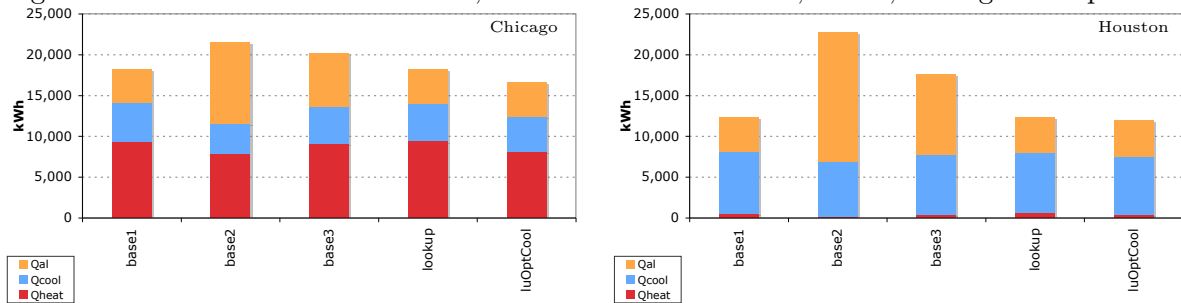


Figure 31: Comparisons of annual results, internal Venetian blinds, South, Chicago lookup

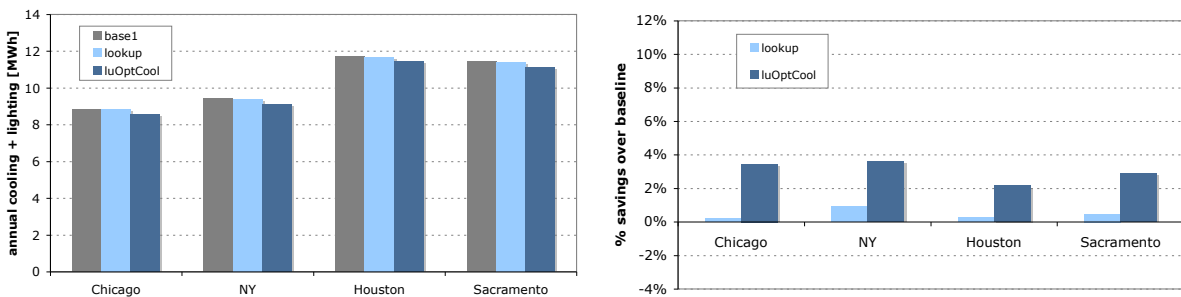
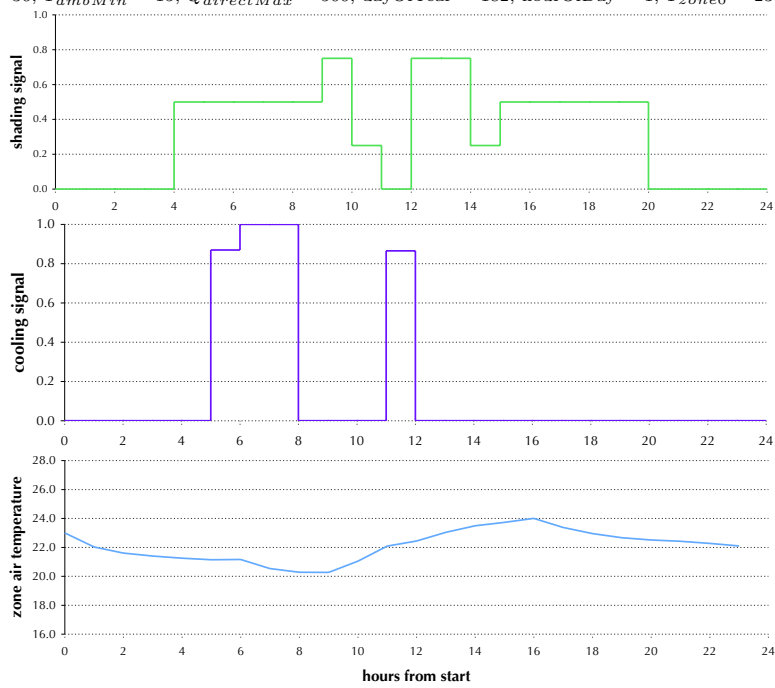


Table 9: Percent savings relative to Base1, internal Venetian blinds, South, Chicago lookup

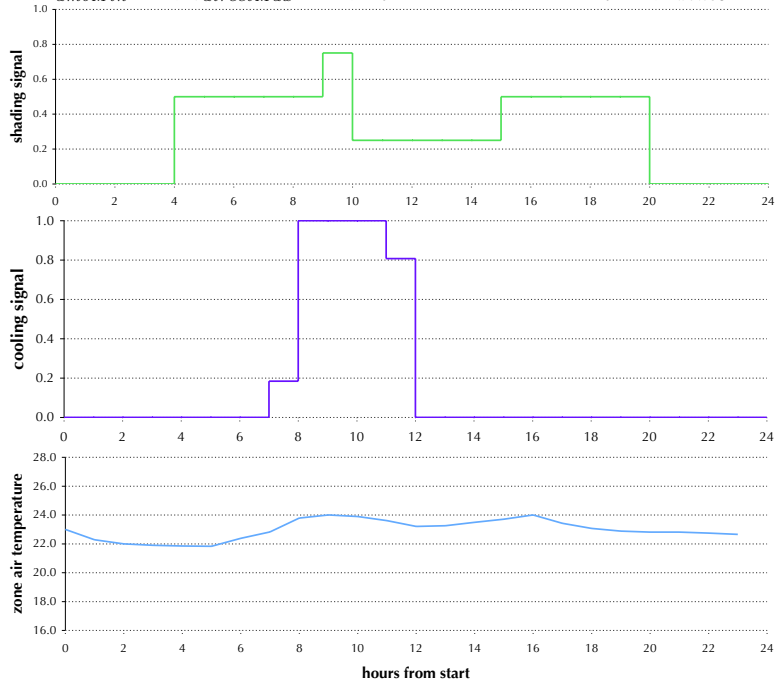
	Chicago			NY			Houston			Sacramento		
	light	cool	total	light	cool	total	light	cool	total	light	cool	total
lookup	-3.1	3.1	0.2	-2.2	3.3	0.9	-4.0	2.7	0.3	-6.4	4.5	0.5
luOptCool	-2.5	8.7	3.5	-2.3	8.0	3.6	-4.2	5.8	2.2	-5.3	7.8	2.9

Figure 32: Examples from control lookup table, internal Venetian blinds, South, Chicago

$\{ T_{ambMax} = 30, T_{ambMin} = 15, \dot{Q}_{directMax} = 500, \text{dayOfYear} = 182, \text{hourOfDay} = 1, T_{zone0} = 23, T_{slab0} = 21 \}$



$\{ T_{ambMax} = 30, T_{ambMin} = 20, \dot{Q}_{directMax} = 500, \text{dayOfYear} = 182, \text{hourOfDay} = 1, T_{zone0} = 23, T_{slab0} = 21 \}$



4.4 Electrochromic windows, South zone

4.4.1 Control lookup table

Figure 35 shows two example points in the control lookup table.

4.4.2 Annual simulation results

The annual simulation results are summarized in Figures 33 and 34, and in Table 10. In the Base1 and Base3 cases the open state is 0.75 (3/4 darkened).⁴ The results here differ from the other cases in that the lighting savings relative to Base1 are positive and the cooling savings negative; the controllers save lighting energy over Base1 by using less dark states more often, suggesting that either the Base1 shading level is somewhat darker than it should be, or that constant values work less well for electrochromics than for Venetian blinds. (More work is needed to determine what went wrong in the Sacramento case.)

Figure 33: Annual results summaries, electrochromic windows, South, Chicago lookup

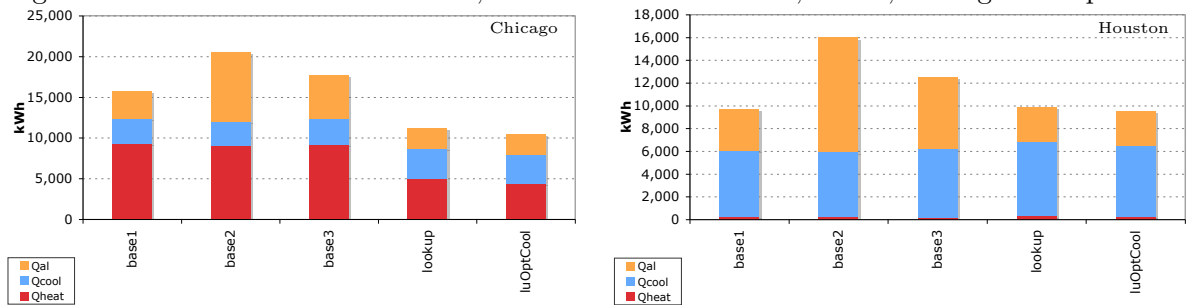


Figure 34: Comparisons of annual results, electrochromic windows, South, Chicago lookup

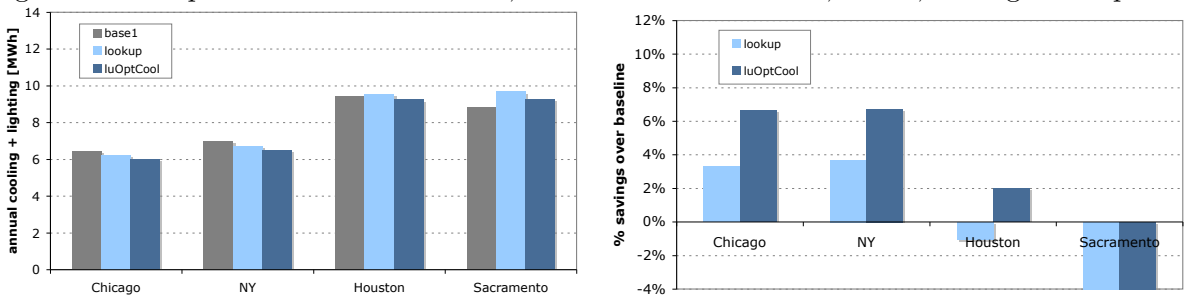


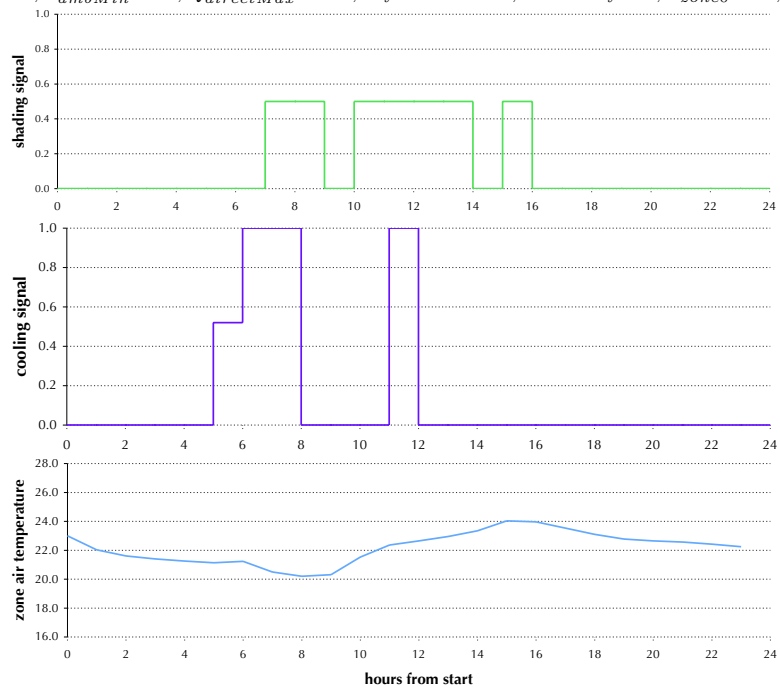
Table 10: Percent savings relative to Base1, electrochromic windows, South, Chicago

lookup	Chicago			NY			Houston			Sacramento		
	light	cool	total	light	cool	total	light	cool	total	light	cool	total
lookup	25.8	-21.5	3.3	25.3	-16.7	3.7	16.5	-11.8	-1.0	10.9	-24.5	-9.7
luOptCool	26.1	-14.9	6.6	25.1	-10.6	6.7	16.6	-7.0	2.0	14.8	-19.0	-4.9

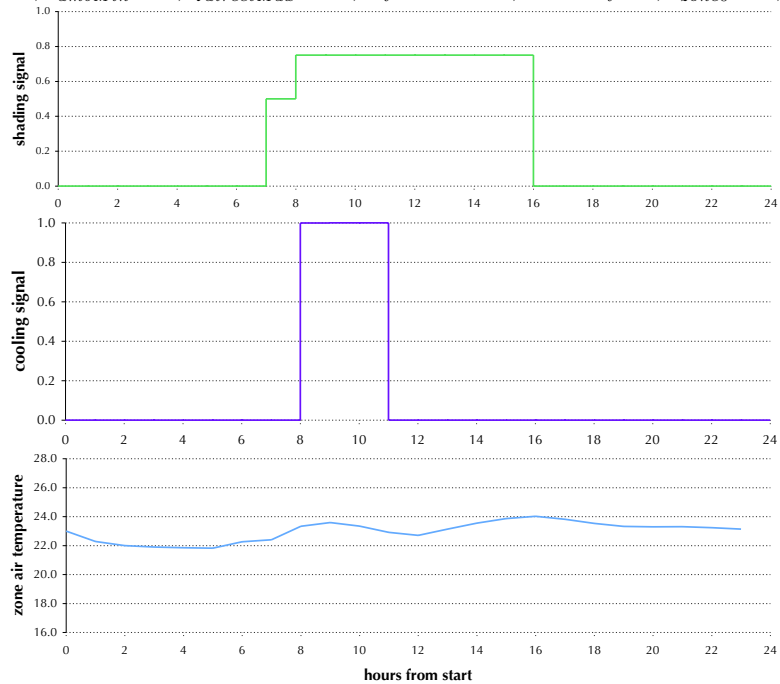
⁴Initial studies with constant values of 0 and 0.5 found that base1 was using significantly more cooling energy and thus performing much worse than the case with this value set to 0.75.

Figure 35: Examples from control lookup table, electrochromic windows, South, Chicago

$\{ T_{ambMax} = 30, T_{ambMin} = 15, \dot{Q}_{directMax} = 500, \text{dayOfYear} = 182, \text{hourOfDay} = 1, T_{zone0} = 23, T_{slab0} = 21 \}$



$\{ T_{ambMax} = 30, T_{ambMin} = 20, \dot{Q}_{directMax} = 500, \text{dayOfYear} = 182, \text{hourOfDay} = 1, T_{zone0} = 23, T_{slab0} = 21 \}$



4.5 Results summary

The annual lighting + cooling savings are summarized in Figures 36 and 37, and in Table 11. The results show greater savings potential for external Venetian blinds than for internal Venetian blinds, as was expected. The results also show greater savings for the South zone than for the West zone. The results for the electrochromic windows show reasonably good savings in Chicago and New York, but less so in Houston and Sacramento - there may be an error in the Sacramento simulation that is causing its very poor performance, but the Houston case could possibly be explained by the Base1 configuration being particularly well-suited to the Houston climate but less well-suited for the Chicago and New York climates, and/or that the Chicago-based control lookup table could not be well applied to the Houston case but it could be to the New York case.

For the external Venetian blinds South cases, the annual lighting + cooling savings are in the range of -0.3% to 4.8% when using the lookup table for both shading and cooling, and in the range of 2.4% to 7.3% when using the lookup table for the shading position and an online optimization for the cooling. For the external Venetian blinds West cases, the savings are in the range of -0.3% to 0.3% and 1.7% to 3.0%. For the internal Venetian blinds South cases, the savings are in the range of 0.2% to 0.9% and 2.2% to 3.6%. For the electrochromic South cases, not counting the questionable Sacramento results, the savings are in the range of -1.0% to 3.7% and 2.0% to 6.7%.

Figure 36: Comparisons of annual energy graphs

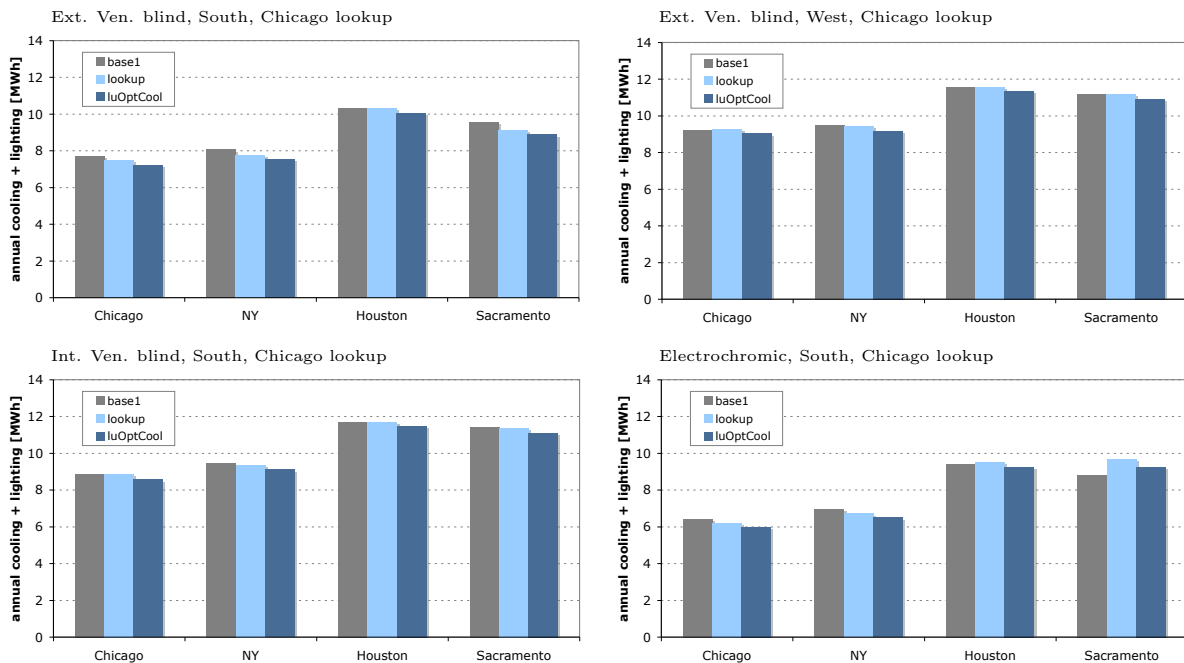


Figure 37: Comparisons of annual lighting + cooling savings graphs

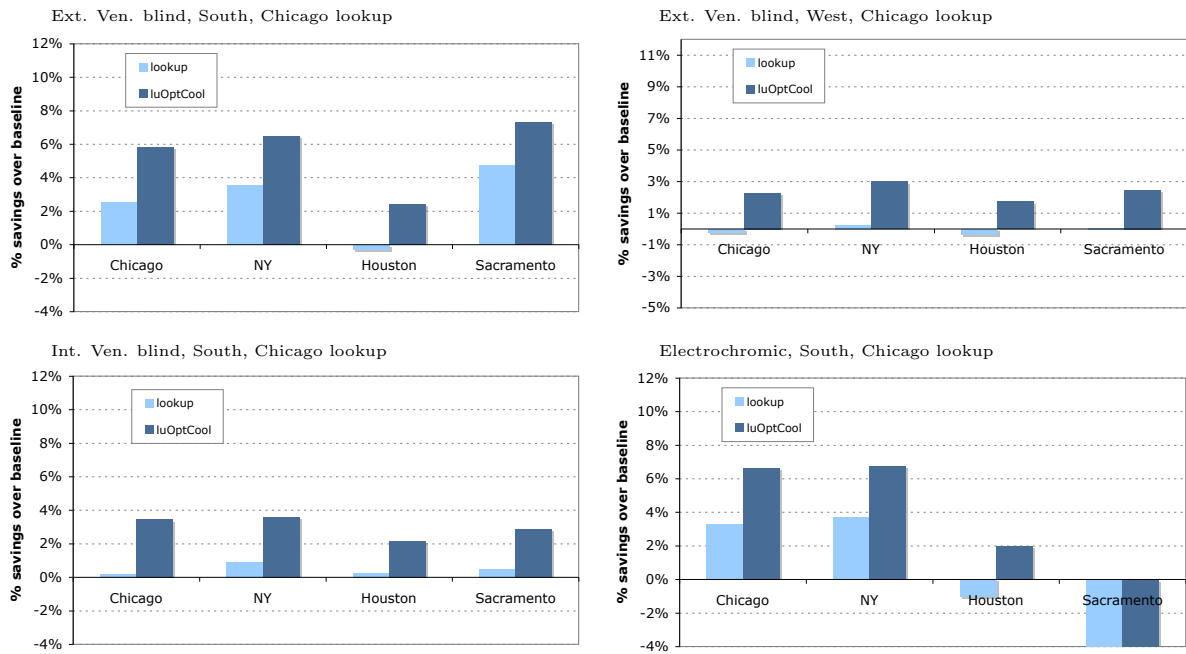


Table 11: Summary of annual lighting + cooling percent savings versus Base1

		Chicago	New York	Houston	Sacramento
External Venetian blinds, South	lookup	2.6	3.5	-0.3	4.8
	luOptCool	5.8	6.5	2.4	7.3
External Venetian blinds, West	lookup	-0.2	0.3	-0.3	0.1
	luOptCool	2.3	3.0	1.7	2.5
Internal Venetian blinds, South	lookup	0.2	0.9	0.3	0.5
	luOptCool	3.5	3.6	2.2	2.9
Electrochromic windows, South	lookup	3.3	3.7	-1.0	-9.7
	luOptCool	6.6	6.7	2.0	-4.9

5 Discussion

5.1 Annual simulation results

The annual simulation results are showing somewhat lower energy savings with optimization-based integrated control than one may have hoped or expected. Some of this may be because there is less savings potential inherent in the problem than one may have hoped, but some may also be because of imperfections in the methods or their implementation. There are reasons to suspect that there may still be minor bugs in the implementation (the annual electrochromic results in Sacramento and the Houston-based lookup table for South-facing external Venetian blinds both suggest there might still be problems left to fix), but it is unexpected that the majority of the optimizations and simulations are in error - their results relative to one another generally make sense.

The process using offline optimization to calculating a control lookup table rather than using online optimization directly in real-time does result in a decrease in performance because of the conditions parametrization and lookup table interpolation (in the case studies in [Coffey, 2011] this performance loss ranged from roughly 10-40%). Estimating the extent of this performance loss in this case could be done by simulating particular weeks or months with online MPC. Interrogating the results of this comparison could also be used to determine how best to refine the control lookup table grid for better performance. It is expected, however, that the results with online optimization would be only slightly better than the results of the ‘luOptCool’ annual simulations, which used online optimization for the cooling part of the problem - the performance difference between the ‘lookup’ case and the ‘luOptCool’ case is likely greater than the performance difference between ‘luOptCool’ and full-online-optimization would be. It seems reasonable to assume, then, that a full-online-optimization case for South-facing external Venetian blinds in Chicago (compared to the ‘lookup’ savings of 2.6% and the ‘luOptCool’ savings of 5.8%) would show annual cooling + lighting savings of somewhere between 5.8% and 9.0% over the base case. Improvements to the control lookup table (e.g. a more refined grid) would also bring some improvements within this range, while still getting the practical benefits of the lookup table. More significant improvements in either the online optimization or lookup table versions may be possible with a higher precision in the shading optimization, as discussed below.

The question of how much higher the savings could be with closer-to-optimal control is thus a difficult question to answer, but it is expected that they would be no more than double the savings shown in the ‘luOptCool’ case. In terms of practical implementation though, only small improvements on the results shown herein would be expected through refinements to the controller.

5.2 Methods

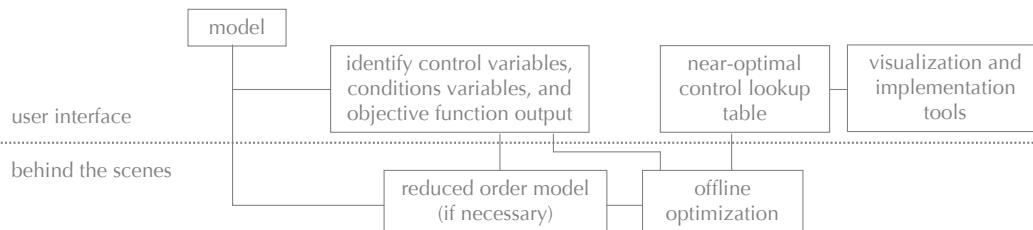
5.2.1 Possible refinements to the controllers

As noted above, refinements to the conditions grid could produce better control performance. However, the biggest improvements at this point would likely come from the use of a more precise optimization for the shading control. The results shown above are for a precision of just 0.25, which is just 5 possible positions of the shade. Increasing the optimization precision, however, would add computational expense to an already expensive computation. One approach might be to use a higher precision for the shading control only for the first few hours of the prediction horizon (likely only for the controller timestep length), and keeping the lower precision for the remaining variables.

5.2.2 Automating the methods for further studies and/or for market implementation

With an eye to automating these methods as much as possible, both to facilitate the analysis of various systems and climates in this project, and to make the process more feasible for other researchers and/or building designers, the overall methods may be described from a user's perspective as illustrated in Figure 38.

Figure 38: MPC tool vision



Within the generic scheme shown in Figure 38, there may be a library of reduced-order models, each applicable to a different type of problem (for which the original model is too slow-running for the control optimization problem given).

Given the calibrated model, it can then be put through the process of conditions grid definition and solution, producing the desired control lookup table. Having gone through the whole process with the case studies, it is now largely automated, and since only the parameter values of the the calibrated model change between cases and all else remains the same, it should be easy to replicate the process for other cases. A few additional scripts could also help to decrease some of the handling between steps.

5.3 Other fenestration and HVAC systems to consider

The types of fenestration and HVAC systems to which MPC can be applied include at least three broad categories:

1. configurations without significant thermal mass (e.g. the NY Times case study)
2. configurations with significant thermal mass in the building and/or HVAC system but not in the facade system (e.g. the case studies herein)
3. configurations with significant thermal mass within the facade system, with or without significant mass in the rest of the building or HVAC system

Type 2 is of particular interest, as it includes a variety of market-available systems, including internal and external shades, electrochromic glazing, other complex fenestration systems, night-flush natural ventilation and massive-slab radiant cooling, and it is more likely than Type 1 to show significant savings potential with MPC. Some of these configurations have been considered herein, others could be relatively easily considered through extensions to the model and methods used herein. The study of Type 3 is more exploratory, searching for significant savings potential that could bolster the development of new component facade technologies - it could include external blinds with facade-embedded phase change materials or thermal mass between layers of variable insulation.

5.4 Further research

- Complete the mapping of savings potential for North American climates
- Add more cases to the ‘no significant thermal mass’ type
- Study examples of active mass in facade
- More extensive coverage of climates
- Get tools into hands of more researchers, designers and product developers
- Develop user interfaces (both scripting-based and graphic-based) to allow user to develop optimization-based control lookup tables given their building / system model, with a minimum number of steps and the details (of the optimization and the reduced-order calibrations, etc) encapsulated such that they need not deal with them if they do not want to
- Use these tools to develop more innovative fenestration-HVAC coupled systems
- Given the map of savings potential, identify promising areas for system design and development
- Work with building designers and product developers on case studies in these promising areas

6 Conclusions

Methods for near-optimal integrated control of operable facades and thermally-massive radiant slabs have been developed. The methods are now mostly automated and can be automated further. The underlying model allows for the consideration of fenestration systems of any arbitrary level of complexity. Initial annual simulation studies with external Venetian blinds, internal Venetian blinds and electrochromic windows, coupled with radiant cooling systems, show modest energy savings, generally in the range of 2-6% of the combined cooling and lighting energy. Further refinement to the controllers may produce slightly better performance, but it is expected to be bounded within the range of 5-10% for these fenestration systems coupled with radiant cooling. The relatively modest savings potential, however, could be offset by the relative ease with which the methods could be automated and used in practical implementations, with the control lookup table used both within design simulation and within the physical implementation. The methods may also be applied to a variety of other types of fenestration-HVAC coupled systems; further investigation may uncover more significant savings potential with more innovative fenestration-HVAC systems.

7 Acknowledgments

This work was supported by the Assistant Secretary for Energy Efficiency and Renewable Energy, Office of Building Technology, State and Community Programs, Office of Building Research and Standards of the U.S. Department of Energy under Contract No. DE-AC02-05CH11231 and by the California Energy Commission through its Public Interest Energy Research (PIER) Program on behalf of the citizens of California.

References

- J Braun. Reducing energy costs and peak electrical demand through optimal control of building thermal storage. *ASHRAE Transactions*, 96(2):264–273, 1990.
- J Clarke, J Crockroft, S Conner, J Hand, N Kelly, R Moore, T O’Brien, and P Strachan. Simulation-assisted control in building energy management systems. *Energy and Buildings*, 34(933-940), 2002.
- B Coffey. Using building simulation and optimization to calculate lookup tables for control. *PhD Thesis, University of California Berkeley*, 2011.
- B Coffey and E Lee. Model-based controls for integrated shading and UFAD control at the New York Times Building: Report on initial studies. *DOE report, Sept*, 2011.
- B Coffey, F Haghghat, E Morofsky, and E Kutrowski. A software framework for model predictive control with GenOpt. *Energy and Buildings*, 42:1084–1092, 2010.
- Z Cumali. Global optimization of HVAC system operations in real time. *ASHRAE Transactions*, 94(1):1729–44, 1988.
- ETH-Zurich. OptiControl project. <http://www.opticontrol.ethz.ch/>, 2011.
- B Flake. Parameter estimation and optimal supervisory control of chilled water plants. *PhD Thesis, University of Wisconsin-Madison*, 1998.
- D Gyalistras and M Gwerder. Use of weather and occupancy forecasts for optimal building climate control (OptiControl): Two years progress report. *Terrestrial Systems Ecology ETH Zurich, Switzerland and Building Technologies Division, Siemens Switzerland Ltd., Zug, Switzerland, 158 pp, Appendices. ISBN 978-3-909386-37-6*, 2010.
- G Henze and M Krarti. Predictive optimal control of active and passive building thermal storage inventory: Final report. *DOE Award Number: DE-FC-26-01NT41255*, 2005.
- G Henze and S Liu. Calibration of building models for supervisory control of commercial buildings. *Proceedings of the 9th International Building Performance Simulation Association (IBPSA) Conference, Montreal, Canada*, 2005.
- G Henze, D Kalz, C Felsmann, and G Knabe. Impact of forecasting accuracy on predictive optimal control of active and passive building thermal storage inventory. *HVAC&R Research*, 10(2):153–177, 2004.
- G Henze, D Kalz, S Liu, and C Felsmann. Experimental analysis of model-based predictive optimal control for active and passive thermal storage inventory. *HVAC&R Research*, 11(2):189–213, 2005.

- J House and T Smith. Optimal control of building and HVAC systems. *Proceedings of the American Control Conference*, 1996.
- IBPSA-USA and IBPSA-Canada. Model Predictive Control in Buildings Workshop, Montreal. <http://www.ibpsa.us/MPCinBuildingsWorkshopProgram.pdf>, 2011.
- K Keeney and J Braun. A simplified method for determining optimal cooling control strategies for thermal storage in building mass. *HVAC&R Research*, 2(1):59–78, 1996.
- M Kummert and P Andre. Simulation of a model-based optimal controller for heating systems under realistic hypotheses. *Proceedings of the 9th International Building Performance Simulation Association (IBPSA) Conference, Montreal, Canada*, 2005.
- M Kummert, P Andre, and A Argigiou. Performance comparison of heating control strategies combining simulation and experimental results. *Proceedings of the 9th International Building Performance Simulation Association (IBPSA) Conference, Montreal, Canada*, 2005.
- Y Ma, F Borrelli, B Hancey, B Coffey, S Bengea, and P Haves. Model predictive control for the operation of building cooling systems. *IEEE Trans. Control Systems Technology*, 20(3):796–803, 2010.
- A Mahdavi. Simulation-based control of building systems operation. *Building and Environment*, 36:789–796, 2001.
- A Mahdavi and C Proglhof. A model-based method for the integration of natural ventilation in indoor climate systems operation. *Proceedings of the 9th International Building Performance Simulation Association (IBPSA) Conference, Montreal, Canada*, 2005.
- A Mahdavi, B Spasojevic, and K Brunner. Elements of a simulation-assisted daylight-responsive illumination systems control in buildings. *Proceedings of the 9th International Building Performance Simulation Association (IBPSA) Conference, Montreal, Canada*, 2005.
- MathWorks. Model predictive control toolbox. <http://www.mathworks.com/products/mpc/>, 2012.
- P May-Ostendorp, G Henze, C Corbin, and B Rajagopalan. Model-predictive control of mixed-mode buildings with rule extraction. *Building and Environment*, 46(2):428–437, 2011.
- D Mayne, J Rawlings, C Rao, and P Scokaert. Constrained model predictive control: Stability and optimality. *Automatica*, 36(6):789–814, 2000.
- M Morari and J Lee. Model predictive control: past, present and future. *Computers and Chemical Engineering*, 23:667–682, 1999.

- N Nassif, S Kajl, and R Sabourin. Simplified model-based optimal control of VAV air-conditioning system. *Proceedings of the 9th International Building Performance Simulation Association (IBPSA) Conference, Montreal, Canada, 2005a*.
- N Nassif, K Stainslaw, and R Sabourin. Optimization of HVAC control system strategy using two-objective genetic algorithm. *HVAC&R Research*, 11(3):459–486, 2005b.
- F Oldewurtel, D Gyalistras, M Gwerder, C Jones, A Parisio, V Stauch, B Lehmann, and M Morari. Increasing energy efficiency in building climate control using weather forecasts and model predictive control. *Clima - RHEVA World Congress, Antalya, Turkey, 2010*.
- S Qin and T Badgwell. A survey of industrial model predictive control technology. *Control Engineering Practice*, 11:733–764, 2003.
- CJ Sloup, D Karnes, and G Henze. Real-time global optimization of building setpoints and sequence of operation. *US Patent No. 7,894,943 B2*, 2011.
- S Wang and X Jin. Model-based optimal control of VAV air-conditioning system using genetic algorithm. *Building and Environment*, 35:471–487, 2000.
- M Wetter. GenOpt: Generic optimization program. <http://gundog.lbl.gov/GO/>, 2009.